Mass spectra of singly heavy baryons in the relativized quark model with heavy-quark dominance*

Zhen-Yu Li (李振宇)^{1,4†} Guo-Liang Yu (于国梁)^{2‡} Zhi-Gang Wang (王志刚)² Jian-Zhong Gu (顾建中)^{3‡} Hong-Tao Shen (沈洪涛)^{4‡}

¹School of Physics and Electronic Science, Guizhou Education University, Guiyang 550018, China
 ²Department of Mathematics and Physics, North China Electric Power University, Baoding 071003, China
 ³China Institute of Atomic Energy, Beijing 102413, China
 ⁴Guangxi Key Lab of Nuclear Physics and Technology, Guangxi Normal University, Guilin 541006, China

Abstract: The rigorous calculation of the spin-orbit terms in a three-quark system is realized based on the Gaussian expansion method and the infinitesimally-shifted Gaussian basis functions in the framework of the relativized quark model, by ignoring the mixing between different excited states. Then, the complete mass spectra of the singly heavy baryons are obtained rigorously, under the heavy-quark dominance mechanism. Accordingly, systematical analyses are performed for the reliability and predictive power of the model, the fine structure of the singly heavy baryon spectra, the assignments of the excited baryons, and some important topics about heavy baryon spectroscopy, such as the missing states, "spin-orbit puzzle," and clustering effect. The results confirm that, under the heavy-quark dominance mechanism, the relativized quark model can describe the excitation spectra and the fine structures of the singly heavy baryons correctly and precisely.

Keywords: singly heavy baryon, spin-orbit interactions, heavy-quark dominance, fine structure, relativized quark model

DOI: 10.1088/1674-1137/adf178 **CSTR:** 32044.14.ChinesePhysicsC.49113107

I. INTRODUCTION

Heavy baryon spectroscopy is crucial for gaining deeper insights into the strong interaction in the non-perturbative regime of quantum chromodynamics (QCD) [1]. It has attracted considerable experimental and theoretical attention. To date, numerous singly heavy baryons have been observed in experiments [2–22], providing important support for related theoretical studies [23–25].

In the new Review of Particle Physics (RPP) by the Particle Data Group (PDG), more than 70 singly heavy baryons have been collected [2]. These heavy baryons and their J^P values are listed in Table 1, which shows that most of the ground states of the heavy baryons have been well established in experiment. However, the J^P

values of several excited baryons have not been identified. Moreover, some of the excited baryons were observed experimentally in groups, and their mass values are very close to each other, such as $\{\Omega_c^0(3000), \Omega_c^0(3050), \Omega_c^0(3090), \Omega_c^0(3120)\}$, $\{\Xi_c(2923)^0, \Xi_c(2930)^{+,0}, \Xi_c(2970)^{+,0}\}$, and $\{\Omega_b(6316)^-, \Omega_b(6330)^-, \Omega_b(6340)^-, \Omega_b(6350)^-\}$. These close mass values in each group indicate a fine structure in their excitation spectra, which is, however, an unsolved problem in the current theory. In addition, as shown in Table 1, several excited heavy baryons have been observed in the last few years, owing to the improvement of experimental accuracy by some collaborations, such as the LHCb, Belle, and CMS. Very recently, a new charmed baryon $\Xi_c(2923)^+$ has been first observed by the LHCb collaboration [22]. It is expected

Received 21 May 2025; Accepted 15 July 2025; Published online 16 July 2025

^{*} Supported by the Open Project of Guangxi Key Lab of Nuclear Physics and Technology (NLK2023-04), the Central Government Guidance Funds for Local Scientific and Technological Development in China (Guike ZY22096024), the Natural Science Foundation of Guizhou Province-ZK[2024](General Project)650, the National Natural Science Foundation of China (11675265, 12175068), the Continuous Basic Scientific Research Project (WDJC-2019-13) and the Leading Innovation Project (LC 192209000701)

[†] E-mail: zhenyvli@163.com

[‡] E-mail: yuguoliang2011@163.com

[§] E-mail: zgwang@aliyun.com

E-mail: gujianzhong2000@aliyun.com

[#] E-mail: shenht@gxnu.edu.cn

Content from this work may be used under the terms of the Creative Commons Attribution 3.0 licence. Any further distribution of this work must maintain attribution to the author(s) and the title of the work, journal citation and DOI. Article funded by SCOAP³ and published under licence by Chinese Physical Society and the Institute of High Energy Physics of the Chinese Academy of Sciences and the Institute of Modern Physics of the Chinese Academy of Sciences and IOP Publishing Ltd

Table 1. Observed singly heavy baryons and their J^P values [2]. $\Sigma_c(2846)^0$ and $\Xi_c(2923)^+$ are cited from Ref. [5] and Ref. [22], respectively.

Baryon	J^P	Baryon	J^P	Baryon	J^P	Baryon	J^P	Baryon	J^P	Baryon	J^P	Baryon	J^P	Baryon	J^P
Λ_c^+	$\frac{1}{2}^{+}$	$\Sigma_c(2455)^{++}$	$\frac{1}{2}^{+}$	Ξ_c^+	$\frac{1}{2}^{+}$	Ω_c^0	$\frac{1}{2}^{+}$	Λ_b^0	$\frac{1}{2}^{+}$	Σ_b^+	$\frac{1}{2}^{+}$	Ξ_b^0	$\frac{1}{2}^{+}$	Ω_b^-	1+
$\Lambda_c(2595)^+$	$\frac{1}{2}^{-}$	$\Sigma_c(2455)^+$	$\frac{1}{2}^{+}$	Ξ_c^0	$\frac{1}{2}^{+}$	$\Omega_c(2770)^0$	$\frac{3}{2}^{+}$	$\Lambda_b(5912)^0$	$\frac{1}{2}^{-}$	Σ_b^-	$\frac{1}{2}^{+}$	Ξ_b^-	$\frac{1}{2}^{+}$	$\Omega_b(6316)^-$??
$\Lambda_c(2625)^+$	$\frac{3}{2}^{-}$	$\Sigma_c(2455)^0$	$\frac{1}{2}^{+}$	$\Xi_c^{'+}$	$\frac{1}{2}^{+}$	$\Omega_c(3000)^0$??	$\Lambda_b(5920)^0$	$\frac{3}{2}^{-}$	Σ_b^{*+}	$\frac{1}{2}^{+}$ $\frac{3}{2}^{+}$ $\frac{3}{2}^{+}$	$\Xi_b(5935)^-$	$\frac{1}{2}^{+}$	$\Omega_b(6330)^-$??
$\Lambda_c(2765)^+$??	$\Sigma_c(2520)^{++}$	$\frac{3}{2}^{+}$	$\Xi_c^{\prime0}$	$\frac{1}{2}^{+}$	$\Omega_c(3050)^0$??	$\Lambda_b(6070)^0$	$\frac{1}{2}^{+}$	Σ_b^{*-}	$\frac{3}{2}^{+}$	$\Xi_b(5945)^0$	$\frac{3}{2}^{+}$	$\Omega_b(6340)^-$??
$\Lambda_c(2860)^+$	$\frac{3}{2}^{+}$	$\Sigma_c(2520)^+$	$\frac{3}{2}^{+}$	$\Xi_c(2645)^+$	$\frac{3}{2}^{+}$	$\Omega_c(3065)^0$??	$\Lambda_b(6146)^0$	$\frac{3}{2}^{+}$	$\Sigma_b(6097)^+$??	$\Xi_b(5955)^-$	$\frac{3}{2}^{+}$	$\Omega_b(6350)^-$??
$\Lambda_c(2880)^+$	$\frac{5}{2}^{+}$	$\Sigma_c(2520)^0$	$\frac{3}{2}^{+}$	$\Xi_c(2645)^0$	$\frac{3}{2}^{+}$	$\Omega_c(3090)^0$??	$\Lambda_b(6152)^0$	$\frac{5}{2}^{+}$	$\Sigma_b(6097)^-$??	$\Xi_b(6087)^0$	$\frac{3}{2}^{-}$		
$\Lambda_c(2910)^+$??	$\Sigma_c(2800)^{++}$	$?^{?}$	$\Xi_c(2790)^+$	$\frac{1}{2}^{-}$	$\Omega_c(3120)^0$??					$\Xi_b(6095)^0$	$\frac{3}{2}^{-}$		
$\Lambda_c(2940)^+$	$\frac{3}{2}^{-}$	$\Sigma_c(2800)^+$	$?^{?}$	$\Xi_c(2790)^0$	$\frac{1}{2}^{-}$	$\Omega_c(3185)^0$??					$\Xi_b(6100)^-$	$\frac{3}{2}^{-}$		
		$\Sigma_c(2800)^0$	$?^{?}$	$\Xi_c(2815)^+$	$\frac{3}{2}^{-}$	$\Omega_c(3327)^0$??					$\Xi_b(6227)^0$??		
		$\Sigma_c(2846)^0$	$?^{?}$	$\Xi_c(2815)^0$	$\frac{3}{2}^{-}$							$\Xi_b(6227)^-$	$?^{?}$		
				$\Xi_c(2882)^0$	$?^{?}$							$\Xi_b(6327)^0$	$?^{?}$		
				$\Xi_c(2923)^+$??							$\Xi_b(6333)^0$??		
				$\Xi_c(2923)^0$	$?^{?}$										
				$\Xi_c(2930)^+$??										
				$\Xi_c(2930)^0$??										
				$\Xi_c(2970)^+$	$\frac{1}{2}^{+}$										
				$\Xi_c(2970)^0$	$\frac{1}{2}^{+}$										
				$\Xi_c(3055)^+$	$?^{?}$										
				$\Xi_c(3080)^+$??										
				$\Xi_c(3080)^0$	$?^{?}$										
				$\Xi_c(3120)^+$??										

that more heavy baryons will be observed in the near future, and more fine structures are also expected to be discovered.

These experimental advancements show that it is time to systematically analyze the data and delineate a reliable mass spectrum. However, providing an accurate analysis of these observed heavy baryons theoretically is difficult and has become a considerable challenge for various theoretical methods. As an indispensable tool for understanding the multitude of observed baryons and their properties, the relativized quark model with QCD also faces the same challenge.

The relativized quark model was developed by Godfrey and Isgur in 1985 [26] and has achieved considerable success in analyzing the meson spectra. The Hamiltonian of this model is based on a universal one-gluon-exchange-plus-linear-confinement potential motivated by QCD, which contains almost all possible forms of the main interaction between the two quarks. In 1986,

Capstick and Isgur extended this model, insisted on using the method of studying light-quark baryons, and systematically studied the mass spectra of both light and heavy baryons under a unified framework [27]. Their study in baryon spectroscopy produced a lasting effect [28]. However, their study predicted more "missing" states of the heavy baryons, which is similar to the case of the light-quark baryons. Once more, in a manner similar to that for the light-quark baryons, there are two possible solutions to the problem for the heavy baryons summarized by Capstick and Roberts. The first one is that the dynamical degrees of freedom used in the model, namely, the three valence quarks, are not physically realized. Instead, a baryon consists of a quark and a diquark, and the reduction of the number of internal degrees of freedom leads to a more sparsely populated spectrum. The second possible solution is that the missing states couple weakly to the formation channels used to investigate the states and hence make very small contributions to the scattering cross sections [29].

Later, the heavy quark symmetry [30], heavy quark limit [31], and heavy quark effective theory (HQET) [32, 33] were proposed successively and revealed some important structural properties of the heavy baryons, which laid the foundation for the solution of the above problem. According to the first possible solution, Ebert, Faustov, and Galkin analyzed the spectra of the singly heavy baryons in the heavy quark-light diquark picture [34] and predicted significantly fewer states than those of Ref. [27] mentioned above, which has two important implications. One implication is that the total orbital angular momentum L can be approximatively regarded as a good quantum number of a baryon state, although it is not true strictly in a relativistic theory. In practice, as an approximative good quantum number, L has been widely used in studies [35–43]. The other implication is that the concept of "the clustering effect" is officially applied in the study, which indicates that there might exist a cluster in the singly heavy baryon, if this solution is correct. However, the reliability of the first solution has yet to be tested further. Thus, this simple diagnostic is difficult to apply since information on the excited baryon spectrum is scarce [1].

Inspired by the above related theoretical works, we studied the spectra of the singly and doubly heavy baryons systematically in the framework of the relativized quark model [44-48]. The method used adopted the respective advantages of the above two possible solutions. We considered L to be an approximative good quantum number, assumed that the stable (or physically realized) quantum states for the excited heavy baryons should exist in the lower orbital excitation mode, and further ignored the mixing between different excited states. The results showed that most of the experimental data can be well described with a uniform set of parameters for the heavy baryons. We analyzed the orbital excitation of the heavy baryons carefully and proposed the heavy-quark dominance (HQD) mechanism, which may solve the problem of the "missing" states in a natural way and determine the overall structure of the excitation spectra for the singly and doubly heavy baryons [49].

For describing the fine structure of the observed excited baryons, we improved the calculation of the spin-orbit interactions by considering the contribution from the light-quark cluster in a quasi-two-body spin-orbit interaction, which enhances the energy level splitting of the orbital excitation significantly and presents a reasonable fine structure [50]. The analysis of the fine structure confirms that the contribution of the spin-orbit interaction from the orbital angular momentum I_{λ} is not negligible.

The predicted singly heavy baryon spectra in our studies match well with the current data. However, they are still unsatisfactory because approximate formulas were used for describing the contributions of the spin-or-

bit interaction to the fine structures [50]. Consequently, one cannot judge the deviation from the real results. This reduces the reliability of the calculation and the predictive power. Hence, it is necessary to analyze the fine structure by using a rigorous calculation. However, the rigorous calculation is a common challenge for threebody systems. As the Hamiltonian of the relativized quark model is based on the two-body interaction, one will encounter some technical difficulties in the rigorous calculation, when the model is extended from the mesons to the baryons. This is the biggest obstacle that this model has encountered in studying three-quark systems. If the rigorous calculation is implemented, some important problems of this model appearing in the heavy baryon spectroscopy might be solved, such as the missing states [29], "spin-orbit puzzle" [51, 52], and clustering effect in a heavy baryon. In addition, a more important question could be answered, i.e., whether and how the relativized quark model can correctly describe the heavy baryon spectroscopy.

In this study, we attempted to perform a rigorous calculation of the heavy baryon spectra in the relativized quark model with the HQD mechanism, by using the Gaussian expansion method (GEM) and the infinitesimally-shifted Gaussian (ISG) basis functions [53, 54], to obtain a complete mass spectrum of the singly heavy baryons, answer the questions mentioned above, and provide a reliable analysis for the relative studies.

The remainder of this paper is organized as follows. In Sec. II, the theoretical methods used in this study, including the Hamiltonian of the relativized quark model, wave functions, and Jacobi coordinates, and the evaluations of the matrix elements, including the rigorous calculation of the spin-orbit terms, are introduced. The structural properties of the singly heavy baryon spectra, the comparison between the calculated excitation spectra and the experimental data, and the reliability of the model are analyzed in Sec. III. Finally, Sec. IV presents the conclusions.

II. THEORETICAL METHODS USED IN THIS STUDY

A. Hamiltonian of the relativized quark model

In the relativized quark model, the Hamiltonian for a three-quark system is based on the two-body interactions,

$$H = H_0 + \tilde{H}^{\text{conf}} + \tilde{H}^{\text{hyp}} + \tilde{H}^{\text{so}}$$

$$= \sum_{i=1}^{3} \sqrt{p_i^2 + m_i^2} + \sum_{i < j} \left(\tilde{H}_{ij}^{\text{conf}} + \tilde{H}_{ij}^{\text{hyp}} + \tilde{H}_{ij}^{\text{so}} \right), \qquad (1)$$

where the interaction terms $\tilde{H}_{ij}^{\text{conf}}$, $\tilde{H}_{ij}^{\text{hyp}}$, and $\tilde{H}_{ij}^{\text{so}}$ are the confinement, hyperfine, and spin-orbit interactions, re-

spectively. The confinement term $\tilde{H}_{ij}^{\text{conf}}$ includes a modified one-gluon-exchange potential $G'_{ij}(r)$ and a smeared linear confinement potential $\tilde{S}_{ij}(r)$. The hyperfine interaction $\tilde{H}_{ij}^{\text{hyp}}$ consists of the tensor term $\tilde{H}_{ij}^{\text{tensor}}$ and the contact term \tilde{H}_{ij}^c . The spin-orbit interaction $\tilde{H}_{ij}^{\text{so}}$ can be divided into the color-magnetic term $\tilde{H}_{ij}^{\text{so}(s)}$ and the Thomasprecession term $\tilde{H}_{ij}^{\text{so}(s)}$. Their forms are described in detail below.

$$\begin{split} \tilde{H}_{ij}^{\text{conf}} &= G'_{ij}(r) + \tilde{S}_{ij}(r), \\ \tilde{H}_{ij}^{\text{hyp}} &= \tilde{H}_{ij}^{\text{tensor}} + \tilde{H}_{ij}^{c}, \\ \tilde{H}_{ii}^{\text{so}} &= \tilde{H}_{ii}^{\text{so}(v)} + \tilde{H}_{ii}^{\text{so}(s)}, \end{split} \tag{2}$$

with

$$\tilde{H}_{ij}^{\text{tensor}} = -\frac{\mathbf{s}_{i} \cdot \mathbf{r}_{ij} \mathbf{s}_{j} \cdot \mathbf{r}_{ij} / r_{ij}^{2} - \frac{1}{3} \mathbf{s}_{i} \cdot \mathbf{s}_{j}}{m_{i} m_{j}} \times \left(\frac{\partial^{2}}{\partial r_{ij}^{2}} - \frac{1}{r_{ij}} \frac{\partial}{\partial r_{ij}}\right) \tilde{G}_{ij}^{t}, \tag{3}$$

$$\tilde{H}_{ij}^c = \frac{2\mathbf{s}_i \cdot \mathbf{s}_j}{3m_i m_j} \nabla^2 \tilde{G}_{ij}^c,\tag{4}$$

$$\tilde{H}_{ij}^{\text{so(v)}} = \frac{\mathbf{s}_{i} \cdot \mathbf{L}_{(ij)i}}{2m_{i}^{2} r_{ij}} \frac{\partial \tilde{G}_{ii}^{\text{so(v)}}}{\partial r_{ij}} + \frac{\mathbf{s}_{j} \cdot \mathbf{L}_{(ij)j}}{2m_{j}^{2} r_{ij}} \frac{\partial \tilde{G}_{jj}^{\text{so(v)}}}{\partial r_{ij}} + \frac{(\mathbf{s}_{i} \cdot \mathbf{L}_{(ij)j} + \mathbf{s}_{j} \cdot \mathbf{L}_{(ij)i})}{m_{i} m_{j} r_{ij}} \frac{\partial \tilde{G}_{ij}^{\text{so(v)}}}{\partial r_{ij}},$$
(5)

$$\tilde{H}_{ij}^{\text{so}(s)} = -\frac{\mathbf{s}_i \cdot \mathbf{L}_{(ij)i}}{2m_i^2 r_{ij}} \frac{\partial \tilde{S}_{ii}^{\text{so}(s)}}{\partial r_{ij}} - \frac{\mathbf{s}_j \cdot \mathbf{L}_{(ij)j}}{2m_j^2 r_{ij}} \frac{\partial \tilde{S}_{jj}^{\text{so}(s)}}{\partial r_{ij}}.$$
 (6)

Here, the following conventions are used, *i.e.*, $\mathbf{L}_{(ij)i} = \mathbf{r}_{ij} \times \mathbf{p}_i$ and $\mathbf{L}_{(ij)j} = -\mathbf{r}_{ij} \times \mathbf{p}_j$. In the formulas above, G'_{ij} , \tilde{G}^c_{ij} , \tilde{G}^c_{ij} , \tilde{G}^c_{ij} , $\tilde{G}^{\text{so}(v)}_{ij}$, and $\tilde{S}^{\text{so}(s)}_{ii}$ should be modified with the momentum-dependent factors as follows:

$$G'_{ij} = \left(1 + \frac{p_{ij}^{2}}{E_{i}E_{j}}\right)^{\frac{1}{2}} \tilde{G}_{ij}(r_{ij}) \left(1 + \frac{p_{ij}^{2}}{E_{i}E_{j}}\right)^{\frac{1}{2}},$$

$$\tilde{G}_{ij}^{t} = \left(\frac{m_{i}m_{j}}{E_{i}E_{j}}\right)^{\frac{1}{2}+\epsilon_{t}} \tilde{G}_{ij}(r_{ij}) \left(\frac{m_{i}m_{j}}{E_{i}E_{j}}\right)^{\frac{1}{2}+\epsilon_{t}},$$

$$\tilde{G}_{ij}^{c} = \left(\frac{m_{i}m_{j}}{E_{i}E_{j}}\right)^{\frac{1}{2}+\epsilon_{c}} \tilde{G}_{ij}(r_{ij}) \left(\frac{m_{i}m_{j}}{E_{i}E_{j}}\right)^{\frac{1}{2}+\epsilon_{c}},$$

$$\tilde{G}_{ij}^{so(v)} = \left(\frac{m_{i}m_{j}}{E_{i}E_{j}}\right)^{\frac{1}{2}+\epsilon_{so(v)}} \tilde{G}_{ij}(r_{ij}) \left(\frac{m_{i}m_{j}}{E_{i}E_{j}}\right)^{\frac{1}{2}+\epsilon_{so(v)}},$$

$$\tilde{S}_{ii}^{so(s)} = \left(\frac{m_{i}m_{i}}{E_{i}E_{j}}\right)^{\frac{1}{2}+\epsilon_{so(s)}} \tilde{S}_{ij}(r_{ij}) \left(\frac{m_{i}m_{i}}{E_{i}E_{j}}\right)^{\frac{1}{2}+\epsilon_{so(s)}},$$
(7)

where $E_i = \sqrt{m_i^2 + p_{ij}^2}$ is the relativistic kinetic energy, and p_{ij} is the momentum magnitude of either of the quarks in the center-of-mass frame of the ij quark subsystem [27, 55].

 $\tilde{G}_{ij}(r_{ij})$ and $\tilde{S}_{ij}(r_{ij})$ are obtained by the smearing transformations of the one-gluon exchange potential $G(r) = -\frac{4\alpha_s(r)}{3r}$ and linear confinement potential $S(r) = \tilde{b}r + \tilde{c}$, respectively,

$$\tilde{G}_{ij}(r_{ij}) = \mathbf{F}_i \cdot \mathbf{F}_j \sum_{k=1}^{3} \frac{2\alpha_k}{\sqrt{\pi}r_{ij}} \int_0^{\tau_{kij}r_{ij}} e^{-x^2} dx,$$
 (8)

$$\tilde{S}_{ij}(r_{ij}) = -\frac{3}{4} \mathbf{F}_i \cdot \mathbf{F}_j \left\{ \tilde{b} r_{ij} \left[\frac{e^{-\sigma_{ij}^2 r_{ij}^2}}{\sqrt{\pi} \sigma_{ij} r_{ij}} + \left(1 + \frac{1}{2\sigma_{ij}^2 r_{ij}^2} \right) \frac{2}{\sqrt{\pi}} \int_0^{\sigma_{ij} r_{ij}} e^{-x^2} dx \right] + \tilde{c} \right\},$$
(9)

with

$$\tau_{kij} = \frac{1}{\sqrt{\frac{1}{\sigma_{ij}^2} + \frac{1}{\gamma_k^2}}},$$

$$\sigma_{ij} = \sqrt{s_0^2 \left(\frac{2m_i m_j}{m_i + m_j}\right)^2 + \sigma_0^2 \left[\frac{1}{2} \left(\frac{4m_i m_j}{(m_i + m_j)^2}\right)^4 + \frac{1}{2}\right]}. \quad (10)$$

Here, α_k and γ_k are constants. $\mathbf{F}_i \cdot \mathbf{F}_j$ represents the inner product of the color matrices of quarks i and j. For the baryon, $\langle \mathbf{F}_i \cdot \mathbf{F}_j \rangle = -2/3$. All the parameters in these formulas are consistent with those in our previous studies [44, 45]. Their values are listed in Table 2.

B. Wave functions and Jacobi coordinates

For a singly heavy baryon system, the heavy-quark is decoupled from the two light-quarks in the heavy quark limit. With the requirement of the flavor SU(3) subgroups for the light-quark pair, the singly heavy baryons belong to either a sextet $(\mathbf{6}_F)$ of the flavor symmetric states,

$$\Sigma_{Q} = (uu)Q, \frac{1}{\sqrt{2}}(ud+du)Q, (dd)Q,$$

$$\Xi_{Q}' = \frac{1}{\sqrt{2}}(us+su)Q, \frac{1}{\sqrt{2}}(ds+sd)Q,$$

$$\Omega_{Q} = (ss)Q,$$
(11)

or an anti-triplet $(\bar{\mathbf{3}}_F)$ of the flavor antisymmetric states [33],

$(m_u/m_d)/\text{GeV}$	$m_s/{\rm GeV}$	$m_c/{ m GeV}$	$m_b/{ m GeV}$	γ ₁ /GeV	γ ₂ /GeV	$\gamma_3/{ m GeV}$	$\tilde{b}/{\rm GeV^2}$	~c/GeV
0.22	0.419	1.628	4.977	1/2	$\sqrt{10}/2$	$\sqrt{1000}/2$	0.14	-0.198
ϵ_{c}	ϵ_t	$\epsilon_{SO(v)}$	$\epsilon_{\mathrm{SO}(s)}$	α_1	α_2	α_3	$\sigma_0/{ m GeV}$	ĩ
-0.168	0.025	-0.035	0.055	0.25	0.15	0.20	1.8	1.55

Table 2. Parameters of the relativized quark model in this study. Their values are the same as those in Ref. [26], apart from \tilde{b} and \tilde{c} [44].

$$\Lambda_{Q} = \frac{1}{\sqrt{2}} (ud - du)Q,$$

$$\Xi_{Q} = \frac{1}{\sqrt{2}} (us - su)Q, \frac{1}{\sqrt{2}} (ds - sd)Q. \tag{12}$$

Here, u, d, and s denote up, down, and strange quarks, respectively. Q denotes a charm (c) quark or bottom (b) quark.

For describing the internal orbital motion of the singly heavy baryon, we select the specific Jacobi coordinates (named JC-3 for short) as shown in Fig. 1, which is consistent with the above reservation about the flavor wave function naturally. In this study, the Jacobi coordinates are defined as

$$\rho_{i} = \mathbf{r}_{jk} = \mathbf{r}_{j} - \mathbf{r}_{k},$$

$$\lambda_{i} = \mathbf{r}_{i} - \frac{m_{j}\mathbf{r}_{j} + m_{k}\mathbf{r}_{k}}{m_{j} + m_{k}},$$

$$\mathbf{R}_{i} = \frac{m_{i}\mathbf{r}_{i} + m_{j}\mathbf{r}_{j} + m_{k}\mathbf{r}_{k}}{m_{i} + m_{j} + m_{k}} \equiv \mathbf{0},$$
(13)

where $\{i, j, k\} = \{1, 2, 3\}, \{2, 3, 1\}, \text{ or } \{3, 1, 2\}.$ \mathbf{r}_i and m_i denote the position vector and the mass of the *i*th quark, respectively. $\mathbf{R}_i \equiv \mathbf{0}$ indicates that the kinetic energy of the center of mass is not considered. Specially, for JC-3 in Fig. 1, the following definitions are used in this study: $\rho_3 \equiv \rho$ and $\lambda_3 \equiv \lambda$.

Based on the above discussion and the HQET [31–33], the spin and orbital wave function of a baryon state is assumed to have the coupling scheme

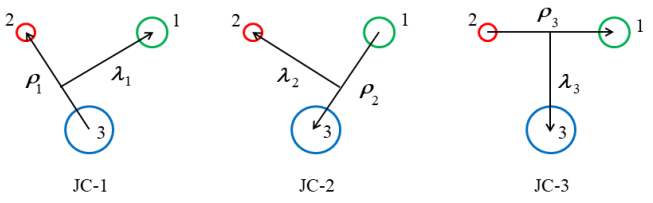


Fig. 1. (color online) Three channels of the Jacobi coordinates for a three-quark system, labeled as $\{\rho_k, \lambda_k\}$ (k=1, 2, 3). The channel 3 (JC-3) is selected for defining the wave function of a singly heavy baryon state. All the quarks are numbered for ease of use in calculations, and the third quark refers specifically to the heavy quark.

$$|(J^P)_j, L\rangle = |\{[(l_\rho l_\lambda)_L (s_1 s_2)_{s_{12}}]_j s_3\}_J\rangle,$$
 (14)

with $P=(-1)^{l_p+l_1}$. $l_p(l_\lambda)$, L, and s_{12} are the quantum numbers of the relative orbital angular momentum l_p (l_λ), total orbital angular momentum L, and total spin of the light-quark pair \mathbf{s}_{12} , respectively. j denotes the quantum number of the coupled angular momentum of L and \mathbf{s}_{12} , so that the total angular momentum $J=j\pm\frac{1}{2}$. More precisely, the baryon state is labeled as $(l_p,l_\lambda)nL(J^P)_j$, in which n is the quantum number of the radial excitation. Such labeling of quantum states is acceptable, especially with L being approximated as a good quantum number [49]. For the Σ_Q , Ξ_Q' , and Ω_Q baryon families, $(-1)^{l_p+s_{12}}=-1$ should be also guaranteed owing to the total antisymmetry of the wave function of the two light quarks, but $(-1)^{l_p+s_{12}}=1$ for the Λ_Q and Ξ_Q families. All conventions are based on JC-3 in Fig. 1.

C. Evaluations of the matrix elements

As the orbital excited state $|\{[(l_{\rho}l_{\lambda})_L(s_1s_2)_{s_1,2}]_js_3\}_J\rangle \equiv$ $|\alpha\rangle_3$ is defined in JC-3 as discussed above, the matrix elements of the Hamiltonian should be evaluated with the wave function $|\alpha\rangle_3$ of the Jacobi coordinates (ρ_3, λ_3) . Here, the subscript 3 represents JC-3. For a given orbital excited state $|\alpha\rangle_3$, the set of Gaussian basis functions $\{|(\tilde{n},\alpha)_3^G\rangle\}$ forms a set of finite-dimensional, non-orthogonal, and complete bases in a finite coordinate (radial) space, which are used in this study to achieve the high precision calculations of the matrix elements. This is the so-called GEM [54]. For the evaluation of the matrix element $\langle (\tilde{n}, \alpha)_3^G | \hat{H}_{ij} | (\tilde{n}', \alpha)_3^G \rangle$ with $\hat{H}_{ij}(r_{ij}) = \hat{H}(\rho_k)$ (k=1, 2, 3corresponds to JC-1, -2, -3, respectively), the Jacobi coordinate transformation needs to be performed as $\{\rho_3, \lambda_3\}$ $\rightarrow \{\rho_k, \lambda_k\}$. However, this will be tedious in the framework of the GEM.

This laborious process can be simplified by introducing the ISG basis functions [54]. With the help of the ISG basis functions, the matrix elements of the Hamiltonian terms H_0 , G'_{ij} , \tilde{S}_{ij} , $\tilde{H}^{\text{tensor}}_{ij}$, and \tilde{H}^c_{ij} could be evaluated rigorously in our previous studies. The GEM and ISG basis functions are briefly introduced in Appendix A and Appendix B, respectively. The detailed results can be found in Ref. [44].

In this study, the rigorous calculation of the spin-orbit terms $\langle (\tilde{n}, \alpha)_3^G | \tilde{H}_{ii}^{SO} | (\tilde{n}', \alpha)_3^G \rangle$ is realized in the frame-

work of the GEM and ISG basis functions, by ignoring the mixing between different excited states. The detailed analysis is presented in Appendix C.

Now, all the Hamiltonian matrix elements are evaluated. The eigenvalues of the Hamiltonian can be obtained rigorously for the orbital excited states and their radial excited states.

III. RESULTS AND DISCUSSIONS

For the *L*-wave excitation with $L=l_{\rho}+l_{\lambda}$, there are an infinite number of orbital excitation modes. Considering L=1 as an example, the excitation modes $(l_{\rho},l_{\lambda})_L$ are $(1,0)_1$, $(0,1)_1$, $(1,1)_1$, $(2,1)_1$, $(1,2)_1$, $(2,2)_1$, etc. We assume that the excitation mode with the lowest energy level is the most stable, has the greatest probability of being observed experimentally, and dominates the structure of the excitation spectrum. This assumption is summarized as the HQD approximation (or the HQD mechanism) [49].

In the HQD mechanism, the orbital excited states of the singly heavy baryons mainly come from the λ -modes $(l_{\rho}=0,l_{\lambda})_{L=l_{\lambda}}$. However, for the *P*-wave orbital excitations of the charm baryons with the $\mathbf{6}_F$ sector, *i.e.*, the Σ_c , Ξ_c' , and Ω_c families, the HQD mechanism is broken because the mass of the *c* quark is not sufficiently high, where both the λ -mode $(0,1)_1$ and the ρ -mode $(1,0)_1$ appear in their *P*-wave states.

Based on the above analyses, the S-, P-, and D-wave states together with their radial excitations of the singly heavy baryons are investigated systematically, and the complete mass spectra are obtained. Considering the Λ_c and Σ_c as examples, the contribution of each Hamiltonian term to the energy levels is given in Table D1 of Appendix D, to show the energy level splitting, the energy level evolution with each Hamiltonian term, and the formation of the fine structures. For the low-lying states, *i.e.*, the 1S-, 2S-, 3S-, 1P-, 2P- (only for the $\overline{\bf 3}_F$ sector), and 1D-wave states in this study, their mass values and the root-mean-square radii are listed in Tables D2–D5 of Appendix D, and the corresponding mass spectra are presented in Fig. 2.

A. Structural properties of singly heavy baryon spectra

(1) Contribution of each Hamiltonian term

In these Hamiltonian terms, $\langle H_{\rm mode} \rangle \equiv \langle H_0 + H^{\rm conf} \rangle$ depends on the excitation modes (l_ρ, l_λ) and dominates the main part of the energy levels. The other terms affect the shift and splitting of the energy levels. This is displayed in Table D1. As shown in Table D1, the tensor terms have little influence on the energy levels. The contact term $\langle H_{12}^c \rangle$ causes a large shift in the energy levels, but has little effect on the energy level splitting. For the Σ_c baryons, the contribution of the contact term $\langle H_{23(31)}^c \rangle$ to the energy level splitting decreases by orders of mag-

nitude with the increase in L.

For the spin-orbit terms, $\langle H_{12}^{\mathrm{SO}(v)} \rangle$ and $\langle H_{12}^{\mathrm{SO}(s)} \rangle$ are equal to 0. The reason is that they are only related to l_{ρ} . In the (0,1) and (0,2) excitation modes $(l_{\rho}=0)$, $\langle H_{12}^{\mathrm{SO}(v)} \rangle$ and $\langle H_{12}^{\mathrm{SO}(s)} \rangle$ vanish. However, in the (1,0) mode $(l_{\rho}=1)$ of the Σ_c baryons, they are still equal to zero because $s_{12}=0$ here, which is constrained by the condition $(-1)^{l_{\rho}+s_{12}}=-1$. Hence, the contribution of the spin-orbit terms comes only from $\langle H_{23}^{\mathrm{SO}(s)} \rangle$ and $\langle H_{23(31)}^{\mathrm{SO}(s)} \rangle$ always partially cancel each other out. However, they jointly lead to the shift and splitting of the energy levels. Particularly in the (1,0) mode, they cause a large splitting of the energy levels, which makes the $(1,0)1P(\frac{1}{2})_1$ state intrude into the region of the (0,1)1P states.

For the energy level splitting, the contribution of the spin-orbit terms is larger than that of the contact terms. Hence, the spin-orbit interaction is important for the excitation spectra structure of the singly heavy baryons.

(2) Heavy-quark dominance

The HQD mechanism and its breaking in the orbital excitation of the heavy baryons were proposed and investigated in Refs. [49, 50]. The HQD mechanism dominates the structure of the excitation spectra. This mechanism indicates that the excitation mode with lower energy levels is always associated with the heavy quark(s), and the splitting of the energy levels is suppressed by the heavy quark(s) as well. In other words, the heavy quarks dominate the orbital excitation of singly and doubly heavy baryons and determine the structures of their excitation spectra. The HQD mechanism is generally effective. However, for the 1P-wave orbital excitation of the singly charm baryons, it is slightly broken, as the c quark is not sufficiently heavy. From Tables D2-D5, the results show that the mechanism remains effective under the rigorous calculation.

(3) Fine structures

As shown in Tables D3–D5 and Fig. 2, the rigorous calculation reveals the perfect fine structures of the excitation spectra, for not only all the 1*P*-wave states but also the 1*D*-wave states of the charm baryons Σ_c , Ξ'_c , and Ω_c . According to the data of the Ω_c baryons, the fine structure of the 1*P*-excited charm baryons $(\Sigma_c, \Xi'_c, \text{ and } \Omega_c)$ should be composed of the five energy levels, which are $(0,1)1P(\frac{1}{2}^-)_{0,1}$, $(0,1)1P(\frac{3}{2}^-)_{1,2}$, $(1,0)1P(\frac{1}{2}^-)_1$ (as an intrude state), $(0,1)1P(\frac{5}{2}^-)_2$, and $(1,0)1P(\frac{3}{2}^-)_1$. However, based on the data of the Ω_b baryons, the fine structure of the 1*P*-wave states of the bottom baryons $(\Sigma_b, \Xi'_b \text{ and } \Omega_b)$ may contain the four energy levels, which are $(0,1)1P(\frac{1}{2}^-)_{0,1}$, $(0,1)1P(\frac{3}{2}^-)_1$, $(0,1)1P(\frac{3}{2}^-)_2$, and $(0,1)1P(\frac{5}{2}^-)_2$. For the 1*D*-wave states of the Σ_c , Ξ'_c , and Ω_c baryons, there are four clear and distinct energy levels as shown in Fig. 2. The

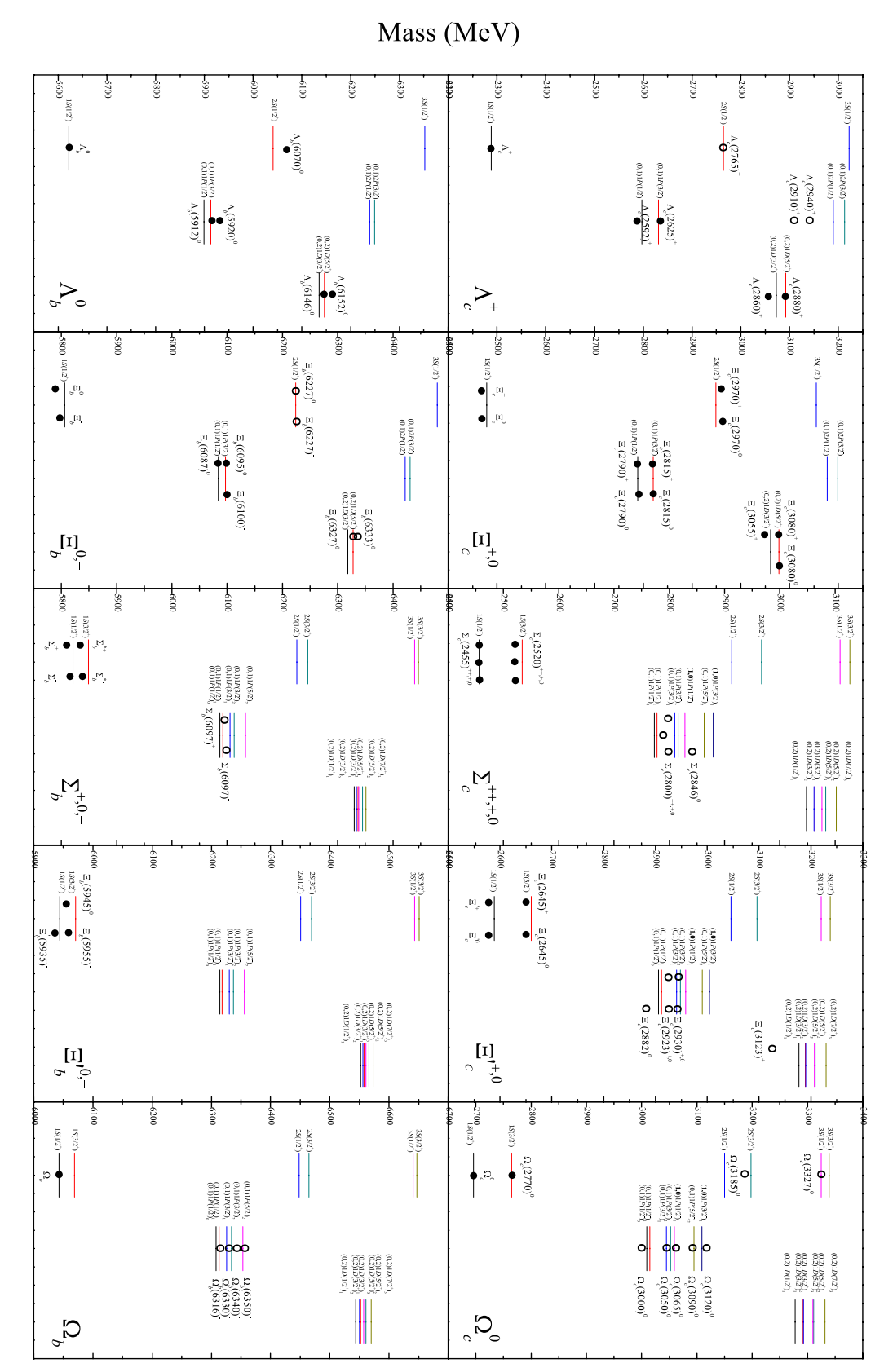


Fig. 2. (color online) Calculated spectra of the singly heavy baryons and the relevant experimental data [2, 5, 22]. "++," "0," and "-" in the brackets indicate the charged states of baryons. The solid black circles denote the baryons with confirmed spin-parity values, and the open circles are the ones whose spin-parities have not been identified.

predicted fine structure of the 1*D*-wave states has yet to be confirmed by future experiments.

(4) Missing states

In the relativized quark model, the calculations in Refs. [27, 28] predicted a substantial number of "missing" states, compared with the experimental observations of the singly heavy baryons. The practice of reducing the internal degrees of freedom, such as the heavy quark-light diquark picture [34], predicted significantly fewer states than the former; however, a reasonable physical explanation is lacking [1, 56]. Now, under the HQD mechanism, the rigorous calculation can reproduce the data well, and the problem of the missing states disappears. Hence, the HQD mechanism in the genuine three-body picture might be a natural solution to the missing states.

(5) Clustering effect

The heavy quark-light diquark picture achieved considerable successes in describing the spectra of the singly heavy baryons, based on an important concept of the "diquark" or quark cluster [34]. By considering the contribution of the quark cluster, the fine structure was preliminarily explained in our previous study [50], which hints that there might be the clustering effect inside a singly heavy baryon. Now, the rigorous calculation shows that, without introducing the concept of the "diquark" or quark cluster, the excitation spectra and their fine structures can also be reproduced very well. Hence, there is no indication that the clustering effect is indispensable inside a singly heavy baryon.

(6) Spin-orbit terms

In both light-quark baryons and heavy-quark baryons, the treatment of the spin-orbit terms used to be a difficult problem [29, 51, 52]. This is mainly due to the following two reasons. One is that the experimental data were not sufficient, and the other is that the rigorous model calculation was difficult. Both difficulties have now been overcome in the research of the singly heavy baryons, i.e., there are sufficient experimental data currently, and the rigorous calculations have been implemented. Table D1 lists the contribution of each spin-orbit term, demonstrating its irreplaceable role in accurately reproducing the fine structures. An earlier assertion is confirmed here, namely, the contribution of the spin-orbit terms must be fully considered before the fine structures can be well explained in the singly heavy baryon spectra [29]. Therefore, based on this study, it is concluded that the spin-orbit terms of the relativized quark model are reasonable for describing the singly heavy baryon spectra, and the "spinorbit puzzle" [29, 51, 52] does not exist anymore here. Note that this study ignores the mixing between different excited states, whose effect on the energy levels needs to be studied further.

B. Excitation spectra and experimental data

In our previous studies, the assignments of the observed baryons were discussed, and a detailed comparison of our results with other theoretical estimations was presented as well [44, 45, 49, 50]. In this study, the rigorous calculation mainly improves the results of the fine structure. Hence, the following discussion focuses on the systematic analysis of the model calculations, by comparing the predicted excitation spectra with the experimental data.

All the observed masses of the singly heavy baryons and the predicted spectra are plotted together in Fig. 2. The detailed experimental data and calculated results are listed in Tables D2–D5, for the $\Lambda_{c(b)}$, $\Xi_{c(b)}$, $\Sigma_{c(b)}$, $\Xi'_{c(b)}$, and $\Omega_{c(b)}$ baryons, respectively. As shown in Fig. 2 and Tables D2–D5, most of the observed masses match well with the predicted spectra, and the maximum deviation between the calculated masses and the data is generally not larger than 20 MeV.

(1) $\Lambda_{c(b)}$ and $\Xi_{c(b)}$ baryons

The $\Lambda_{c(b)}$ and $\Xi_{c(b)}$ baryons belong to the $\bar{\mathbf{3}}_F$ sector. They have the same spectral structure. Fig. 2 shows that the match between the calculation results and the data is good on the whole, except for $\Lambda_c(2910)^+$ and $\Lambda_c(2940)^+$. $\Lambda_c(2940)^+$ was measured by the LHCb collaboration in 2017 [6], and a narrow peak was observed in pD^0 and in $\Lambda_c^+ \pi^+ \pi^-$. It was not observed in pD^+ , and therefore, it might be a Λ_c^+ baryon. Its $J^P = 3/2^-$ is favored but not certain [2]. $\Lambda_c(2910)^+$ was reported by the Belle collaboration in 2022 [17]. It was considered as the candidate of the heavy quark symmetry doublet partner to $\Lambda_c(2940)^+$ [2]. In Fig. 2, these two baryons must be assigned as the 2P-doublet states, if they belong to the Λ_c family. However, the difference between their measured masses and predicted ones is so large that it is far beyond the allowable error range of the theoretical calculation. Hence, $\Lambda_c(2910)^+$ and $\Lambda_c(2940)^+$ are probably not members of the Λ_c family. In some theoretical studies, they were considered as molecular states [35, 57]. However, if only their mass values are considered, they are probably the candidates of the 2S-doublet states in the Σ_c family as shown in Fig. 2 and Table D3. This needs to be further confirmed by experiments.

The $\Xi_b(6227)^{0,-}$ baryons were measured precisely by the LHCb collaboration in 2021 [15], but their J^P values remain unconfirmed. According to their mass values, the $\Xi_b(6227)^{0,-}$ baryons could be assigned as the $2S(\frac{1}{2}^+)$ state of the Ξ_b family as shown in Fig. 2. Alternatively, they might be candidates of the $1P(\frac{1}{2}^-)_{0,1}$ state or the $1P(\frac{3}{2}^-)_1$ state of the Ξ_b' family.

(2) Σ_c and Σ_b baryons

The $\Sigma_c(2800)^{++,+,0}$ baryons were reported by the Belle

Collaboration in 2005 [3]. $\Sigma_c(2846)^0$ was observed by the BaBar collaboration, with $m = 2846 \pm 8 \pm 10$ MeV [5], which has not been collected by the PDG so far. In this study, it is assumed to be a real baryon. Based on the calculation, $\Sigma_c(2846)^0$ and $\Sigma_c(2800)^{++,+,0}$ are in the region of the 1*P*-wave states. By examining their mass values and the fine structure of the 1*P*-wave states shown in Fig. 2, $\Sigma_c(2800)^{++,+,0}$ could be assigned as the $(0,1)1P(\frac{1}{2})_{0,1}$ states, and $\Sigma_c(2846)^0$ could be considered as the intrude state $(1,0)1P(\frac{1}{2})_1$.

The case of $\Sigma_b(6097)^{+,-}$ is similar to that of $\Sigma_c(2800)^{++,+,0}$. Hence, we can conclude that the J^P of $\Sigma_b(6097)^{+,-}$ is likely to be $\frac{1}{2}$. Moreover, they should be the $(0,1)1P(\frac{1}{2})_{0,1}$ states.

(3) Ξ_c' and Ξ_b' baryons

A charged $\Xi_c(2930)^+$ baryon was observed by the Belle collaboration in 2018 [11]. Later, the $\Xi_c(2923)^0$, $\Xi_c(2939)^0$, and $\Xi_c(2964)^0$ states were observed with a large significance by the LHCb collaboration [14]. Very recently, a new charmed baryon $\Xi_c(2923)^+$ was observed for the first time by the LHCb collaboration [22]. In the new PDG data, these baryons were relabeled as $\Xi_c(2923)^0$, $\Xi_c(2930)^{+,0}$, and $\Xi_c(2970)^0$. $\Xi_c(2970)^0$ and its isospin partner $\Xi_c(2970)^+$ are assigned as the $2S(\frac{1}{2}^+)$ state of the Ξ_c family [2]. In contrast, $\Xi_c(2882)^0$ [18], $\Xi_c(2923)^{+,0}$, and $\Xi_c(2930)^{+,0}$ exhibit the fine structure of the 1*P*-wave states in the Ξ_c' family. As shown in Fig. 2, their assignments could be the $(0,1)1P(\frac{1}{2}^-)_{0,1}$, $(0,1)1P(\frac{3}{2}^-)_{1,2}$, and $(1,0)1P(\frac{1}{2}^-)_1$ states, respectively.

 $\Xi_c(3123)^+$ was observed by the BaBar Collaboration in 2007 [4]. It is difficult to make a good assignment for $\Xi_c(3123)^+$. As shown in Fig. 2, we consider it as a candidate of the 1*D*-wave state, although its mass is too small. Alternatively, it could be the $2S(\frac{3}{2}^+)$ state.

If we assume that the $\Xi_b(6227)^{0,-}$ baryons are the strange partners of $\Sigma_b(6097)^{+,-}$, we observe that there are prominent similarities between them. Hence, the $\Xi_b(6227)^{0,-}$ baryons could also be assigned as the same states as $\Sigma_b(6097)^{+,-}$, instead of the $2S(\frac{1}{2}^+)$ state of the Ξ_b family as mentioned above.

(4) Ω_c and Ω_b baryons

For these two families, the predicted fine structures of the 1*P*-wave states reproduce the data perfectly, as shown in Fig. 2. Their assignments are listed in Table D5. $\Omega_c(3185)^0$ is likely to be the $2S(\frac{3}{2}^+)$ state. $\Omega_c(3327)^0$ is assigned as the $3S(\frac{1}{2}^+)$ state, but its mass value overlaps with those of the 1*D*-wave states.

(5) Baryons in the fine structures

 $\Sigma_c(2800)^{++,+,0}$, $\Sigma_c(2846)^0$, and $\Sigma_b(6097)^{+,-}$ have a common feature, *i.e.*, their decay widths are much larger than 15 MeV. However, for the Ξ'_c , Ω_c , and Ω_b baryons in the

fine structures, their decay widths are overall smaller than 15 MeV. Given the similarity in the spectral structures of these $\Sigma_{c(b)}$, $\Xi'_{c(b)}$, and $\Omega_{c(b)}$ families, the decay widths of the baryons in the fine structures could all be small. From this perspective, $\Sigma_c(2800)^{++,+,0}$, $\Sigma_c(2846)^0$, and $\Sigma_b(6097)^{+,-}$ might be the superpositions of several quantum states, and more precise measurements may reveal their fine structures further. $\Xi_b(6227)^{0,-}$ would have the same problem if it belongs to the Ξ'_b family, as well as the assignment of the $\Omega_c(3327)^0$ as mentioned above.

In Ref. [58], the following chain was determined by analyzing the universal behavior of the mass gaps of the baryons:

$$\Sigma_c(2846)^0 \leftrightarrow \Xi_c'(2964)^0 \leftrightarrow \Omega_c(3090)^0,$$
 (15)

which indicates that these baryons are in the same quantum state. Now, $\Xi_c(2964)^0$ (relabeled as $\Xi_c(2970)^0$) is considered as a member of the Ξ_c family. As shown in Fig. 2, the updated chain should be as follows:

$$\Sigma_c(2846)^0 \leftrightarrow \Xi_c'(2930)^0 \leftrightarrow \Omega_c(3065)^0,$$
 (16)

if $\Sigma_c(2846)^0$ is a single state.

C. Reliability of the model

Some approximate calculations were adopted in our previous studies. In Refs. [44, 45], the $\tilde{H}_{13}^{\text{hyp}}$ and $\tilde{H}_{23}^{\text{hyp}}$ terms were ignored in the hyperfine interaction. The spinorbit interaction only contained the $\tilde{H}^{\text{SO}}_{12}$ term coming from the light quark pair and a part of the $\tilde{H}^{\text{SO}}_{d-Q}$ term contributed jointly by the heavy quark (Q) and the lightdiquark (d) (only including the leading order contribution as the Eq. (33) in Ref. [52]). In Ref. [50], the lightdiquark the approximation was considered completely, where the hyperfine interaction was represented by the $\tilde{H}_{12}^{\text{hyp}}$ and $\tilde{H}_{d-Q}^{\text{hyp}}$ terms, and the spin-orbit interaction contained the $\tilde{H}_{12}^{\rm SO}$ and $\tilde{H}_{d-Q}^{\rm SO}$ terms. In this study, all the Hamiltonian terms are obtained without approximation. Consequently, most of the energy levels of the excited states in this study are shifted, even for some of the Swave radial excited states, compared with those in our previous studies.

As the parameters used in the present study are given without any uncertainty, they do not result in any uncertainty in the calculated results. We evaluate the deviations of the calculated masses of the 74 baryons from the measured ones as shown in Table D6. Most of the deviations are less than 20 MeV. The arithmetic average deviation is less than 10 MeV, which is consistent with the estimation result in Ref. [26].

As shown in Fig. 2 and Table D6, the predicted mass spectra in this study can reproduce the data well on the

whole, for all the singly heavy baryon families. The shell structure of the spectra is clearly shown. This indicates that this model can successfully describe the singly heavy baryon spectra without approximation.

The fine structures can be reproduced well, particularly for the Ω_c and Ω_b families. This shows the rationality of the Hamiltonian based on the two-body interactions of the relativized quark model.

However, for the excitation spectrum of each family, there is a slight systematic deviation between the predicted mass values and the data. For a few baryons, such as $\Xi_c(3123)^+$, the theoretical results cannot explain the data reasonably. Hence, some improvements of this model should be attempted, such as a parameter optimization.

In summary, under the HQD mechanism, the relativized quark model can describe the excitation spectra and fine structures correctly. Based on the relativized quark model, the method used in this study should be reliable in research on singly heavy baryon spectroscopy.

IV. CONCLUSIONS

In this study, the rigorous calculation of the spin-orbit terms of the relativized quark model was realized based on the GEM and ISG basis functions, by ignoring the mixing between different excited states. Then, the complete mass spectra of singly heavy baryons were obtained rigorously in the framework of the relativized quark model and under the HQD mechanism. Accordingly, systematical analyses were performed for the reliability and predictive power of the model, the fine structure of the singly heavy baryon spectra, the assignments of the excited baryons, and some important topics about heavy baryon spectroscopy, such as the missing states, clustering effect, and "spin-orbit puzzle."

The main results obtained in the present study are as follows:

- (1) The contribution of each Hamiltonian term to the energy levels was determined.
 - (2) The HQD mechanism was further confirmed.
- (3) The fine structures of the singly heavy baryons were presented.
- (4) The missing states in the singly heavy baryon spectra disappear naturally under the HQD mechanism.
- (5) There was no indication that the clustering effect is indispensable in a singly heavy baryon.
- (6) The spin-orbit terms of the relativized quark model are reasonable for describing the singly heavy baryon spectra, and the "spin-orbit puzzle" does not exist here.

- (7) $\Lambda_c(2910)^+$ and $\Lambda_c(2940)^+$ are probably not members of the Λ_c family. However, they are probably the candidates of the 2*S*-doublet states in the Σ_c family, if only their mass values are considered.
- (8) It was difficult to make a good assignment for the $\Xi_c(3123)^+$ in this study.
- (9) $\Sigma_c(2800)^{++,+,0}$, $\Sigma_c(2846)^0$, and $\Sigma_b(6097)^{+,-}$ may not be single states, and more precise measurements are advised for determining their fine structures further.

In summary, the rigorous calculation shows that, under the HQD mechanism, the relativized quark model can describe the excitation spectra and the fine structures of the singly heavy baryons correctly and precisely. Based on the relativized quark model, the method used in this study should be reliable in research on singly heavy baryon spectroscopy. Furthermore, some improvements of this method should be attempted for a deep understanding of the properties of singly heavy baryon spectroscopy and the strong interaction in the non-perturbative regime of QCD.

ACKNOWLEDGEMENTS

We thank the reviewers for their valuable comments and suggestions. JG would like to thank Professor Yinsheng Ling from Soochow University for his helpful discussion and great encouragement.

APPENDIX

A. Gaussian expansion method (GEM)

Given a set of the orbital quantum numbers $\{l, m\}$, the Gaussian basis function $|(nlm)^G\rangle$ is commonly written in position space as

$$\phi_{nlm}^{G}(\mathbf{r}) = \phi_{nl}^{G}(r) Y_{lm}(\hat{\mathbf{r}}),$$

$$\phi_{nl}^{G}(r) = N_{nl} r^{l} e^{-\nu_{n} r^{2}},$$

$$N_{nl} = \sqrt{\frac{2^{l+2} (2\nu_{n})^{l+3/2}}{\sqrt{\pi} (2l+1)!!}},$$
(A1)

with

$$v_n = \frac{1}{r_n^2}, \quad r_n = r_1 a^{n-1} \quad (n = 1, 2, ..., n_{\text{max}}).$$
 (A2)

 $\{r_1, a, n_{\text{max}}\}\$ (or equivalently, $\{n_{\text{max}}, r_1, r_{n_{\text{max}}}\}\$) are the Gaussian size parameters and commonly related to the scale in question [54]. The optimized values of $\{n_{\text{max}} = 10, r_1 =$

0.18 GeV⁻¹, $r_{n_{\text{max}}} = 15 \text{ GeV}^{-1}$ } are finally selected for the heavy baryons in this study. The details can be found in Refs. [44, 45].

The set $\{\phi_{nlm}^G\}$ forms a set of finite-dimensional, non-orthogonal, and complete bases,

$$N_{n,n'} = \langle \phi_{nlm}^{G} | \phi_{n'lm}^{G} \rangle = \left(\frac{2\sqrt{\nu_{n}\nu_{n'}}}{\nu_{n} + \nu_{n'}} \right)^{l + \frac{3}{2}},$$

$$1 = \sum_{n=1}^{n_{\text{max}}} \sum_{n'=1}^{n_{\text{max}}} |\phi_{nlm}^{G} \rangle (N^{-1})_{nn'} \langle \phi_{n'lm}^{G} |.$$
(A3)

An arbitrary wave function $\psi_{lm}(\mathbf{r})$ can be expanded in a set of definite orbital quantum states,

$$|\psi_{lm}\rangle = \sum_{n,n'=1}^{n_{\text{max}}} |\phi_{nlm}^G\rangle(N^{-1})_{nn'}\langle\phi_{n'lm}^G|\psi_{lm}\rangle \equiv \sum_{n=1}^{n_{\text{max}}} C_n|\phi_{nlm}^G\rangle. \quad (A4)$$

In the definite orbital quantum state, the matrix element of an operator \hat{O} is given by

$$O_{nn'} = \langle \phi_{nlm}^G | \hat{O} | \phi_{n'lm}^G \rangle. \tag{A5}$$

Given $|(nlm)^G\rangle \equiv |n\rangle$ and $|(n'lm)^G\rangle \equiv |n'\rangle$ as well as operators \hat{O}_1 , \hat{O}_2 , and \hat{O}_3 , the matrix element of their inner product in the set of bases is expressed as

$$\langle n|\hat{O}_{1}\hat{O}_{2}\hat{O}_{3}|n'\rangle$$

$$= \sum_{\langle n_{i},n'_{i}\rangle} \langle n|\hat{O}_{1}|n_{1}\rangle (N^{-1})_{n_{1}n'_{1}} \langle n'_{1}|\hat{O}_{2}|n_{2}\rangle (N^{-1})_{n_{2}n'_{2}} \langle n'_{2}|\hat{O}_{3}|n'\rangle$$

$$= \sum_{\langle n_{i},n'_{i}\rangle} (O_{1})_{nn_{1}} (N^{-1})_{n_{1}n'_{1}} (O_{2})_{n'_{1}n_{2}} (N^{-1})_{n_{2}n'_{2}} (O_{3})_{n'_{2}n'}. \tag{A6}$$

Here, $\sum_{\{n_i,n_i'\}}$ indicates sum over all the intermediate indices. The expectation value of an operator \hat{O} in a state $|\alpha\rangle$ is written as

$$\frac{\langle \alpha | \hat{O} | \alpha \rangle}{\langle \alpha | \alpha \rangle} = \frac{\sum_{\{n\}} \langle \alpha | n_1^G \rangle \langle N^{-1} \rangle_{n_1 n_1'} \langle n_1' | \hat{O} | n_2^G \rangle \langle N^{-1} \rangle_{n_2 n_2'} \langle n_2'^G | \alpha \rangle}{\sum_{\{n\}} \langle \alpha | n_3^G \rangle \langle N^{-1} \rangle_{n_3 n_3'} \langle n_3'^G | n_4^G \rangle \langle N^{-1} \rangle_{n_4 n_4'} \langle n_4'^G | \alpha \rangle}$$

$$= \frac{\sum_{\{n\}} C_{n_1'}^* O_{n_1' n_2} C_{n_2}}{\sum_{\{n\}} C_{n_3'}^* N_{n_3' n_4} C_{n_4}}, \tag{A7}$$

in the set of the Gaussian bases.

Now, given a definite quantum state $|(ls)_{JM_J}\rangle$, the generalized Gaussian basis function ($|[n,(ls)_{JM_J}]^G\rangle$) is commonly written as

$$|[n,(ls)_{JM_J}]^G\rangle = \sum_{m_l,m_s} (lm_l sm_s | JM_J) \times |(nlm_l)^G\rangle \otimes |sm_s\rangle. \quad (A8)$$

The set $\{|[n,(ls)_{JM_J}]^G\}$ also forms a set of finite-dimensional, non-orthogonal, and complete bases,

$$N_{n,n'} = \langle [n, (ls)_{JM_J}]^G | [n', (ls)_{JM_J}]^G \rangle = \left(\frac{2\sqrt{\nu_n \nu_{n'}}}{\nu_n + \nu_{n'}}\right)^{l+\frac{3}{2}},$$

$$1 = \sum_{n=1}^{n_{\text{max}}} \sum_{n'=1}^{n_{\text{max}}} |[n, (ls)_{JM_J}]^G \rangle (N^{-1})_{nn'} \langle [n', (ls)_{JM_J}]^G |. \tag{A9}$$

For a singly heavy baryon, we introduce two independent sets of the Gaussian basis functions $|(n_{\rho}l_{\rho}m_{\rho})^{G}\rangle$ and $|(n_{\lambda}l_{\lambda}m_{\lambda})^{G}\rangle$ based on JC-3 in Fig. 1. Given a definite quantum state $|\{[(l_{\rho}l_{\lambda})_{L}(s_{1}s_{2})_{s_{12}}]_{j}s_{3}\}_{JM_{J}}\rangle \equiv |\alpha\rangle_{3}$ (corresponding to JC-3), the generalized Gaussian basis function has the form

$$|(\tilde{n},\alpha)_{3}^{G}\rangle = \sum_{\{m_{\xi}\}} \{CG_{\xi}\} \times |(n_{\rho}l_{\rho}m_{\rho})^{G}\rangle \otimes |(n_{\lambda}l_{\lambda}m_{\lambda})^{G}\rangle$$
$$\otimes |s_{1}m_{s_{1}}\rangle \otimes |s_{2}m_{s_{2}}\rangle \otimes |s_{3}m_{s_{3}}\rangle, \tag{A10}$$

where $\{m_{\xi}\}$ denotes all the third components of the orbital angular momenta and spins, and $\{CG_{\xi}\}$ denotes the products of all the C-G coefficients. \tilde{n} is obtained by combining n_{ρ} and n_{λ} , e.g., $\tilde{n} = (n_{\rho} - 1) \times n_{\max} + n_{\lambda}$ as $n_{\rho(\lambda)} = 1, \dots, n_{\max}$.

The non-orthogonal and complete relations are as follows:

$$\begin{split} N_{\tilde{n},\tilde{n}'} &= \langle (\tilde{n},\alpha)_3^G | (\tilde{n}',\alpha)_3^G \rangle = \left(\frac{2\sqrt{\nu_{n_\rho}\nu_{n_\rho'}}}{\nu_{n_\rho} + \nu_{n_\rho'}} \right)^{l_\rho + \frac{3}{2}} \\ &\times \left(\frac{2\sqrt{\nu_{n_\lambda}\nu_{n_\lambda'}}}{\nu_{n_\lambda} + \nu_{n_\lambda'}} \right)^{l_\lambda + \frac{3}{2}}, \\ 1 &= \sum_{l=1}^{n_{\max}^2} \sum_{l=1}^{n_{\max}^2} |(\tilde{n},\alpha)_3^G\rangle (N^{-1})_{\tilde{n}\tilde{n}'} \langle (\tilde{n}',\alpha)_3^G |. \end{split}$$

In the non-orthogonal representation of $|(\tilde{n}\alpha)_3^G\rangle$, the solution of the eigenenergy E belongs to a generalized matrix eigenvalue problem

$$\sum_{\tilde{n}'=1}^{n_{\max}^2} (H_{\tilde{n}\tilde{n}'} - EN_{\tilde{n}\tilde{n}'})C_{\tilde{n}'} = 0.$$
 (A11)

The matrix element of an operator \hat{H} is given by

$$\begin{split} H_{\tilde{n}\tilde{n}'} &= \langle (\tilde{n}, \alpha)_{3}^{G} | \hat{H} | (\tilde{n}', \alpha)_{3}^{G} \rangle \\ &= \sum_{\{m_{\xi}\}, [m'_{\xi}]} \{ CG_{\xi} \} \times \{ CG_{\xi'} \} \times \langle (n_{\rho}l_{\rho}m_{\rho})^{G} | \langle (n_{\lambda}l_{\lambda}m_{\lambda})^{G} | \\ &\times \langle s_{1}m_{s_{1}} | \langle s_{2}m_{s_{2}} | \langle s_{3}m_{s_{3}} | \hat{H} | s_{1}m'_{s_{1}} \rangle | s_{2}m'_{s_{2}} \rangle | s_{3}m'_{s_{3}} \rangle \\ &\times | (n'_{\rho}l_{\rho}m'_{\rho})^{G} \rangle | (n'_{\lambda}l_{\lambda}m'_{\lambda})^{G} \rangle \\ &\equiv \sum_{\{m_{\xi}, m'_{\xi}\}} \{ CG_{\xi} \times CG_{\xi'} \} \times H_{(n_{\rho}n_{\lambda}, n'_{\rho}n'_{\lambda}); (m_{s_{1,2,3}}, m'_{s_{1,2,3}})}. \end{split}$$
(A12)

The matrix element evaluation of $H_{\tilde{n}\tilde{n}'}$ is finally implemented for $H_{(n_\rho n_\lambda, n'_\rho n'_\lambda);(m_{s_{1,2,3}}, m'_{s_{1,2,3}})}$. For the two-body interaction $\hat{V}_{ij}(r_{ij})$,

$$\begin{split} & [V_{ij}(r_{ij})]_{(n_{\rho}n_{\lambda},n'_{\rho}n'_{\lambda});(m_{s_{1,2,3}},m'_{s_{1,2,3}})} = [V(\rho_{k})]_{(n_{\rho}n_{\lambda},n'_{\rho}n'_{\lambda});(m_{s_{1,2,3}},m'_{s_{1,2,3}})} \\ & \equiv \langle (n_{\rho_{3}}l_{\rho_{3}}m_{\rho_{3}})^{G} | \langle (n_{\lambda_{3}}l_{\lambda_{3}}m_{\lambda_{3}})^{G} | \\ & \times \langle s_{1}m_{s_{1}} | \langle s_{2}m_{s_{2}} | \langle s_{3}m_{s_{3}} | \hat{V}(\rho_{k}) | s_{1}m'_{s_{1}} \rangle | s_{2}m'_{s_{2}} \rangle | s_{3}m'_{s_{3}} \rangle \\ & \times |(n'_{\rho_{3}}l_{\rho_{3}}m'_{\rho_{3}})^{G} \rangle |(n'_{\lambda_{3}}l_{\lambda_{3}}m'_{\lambda_{3}})^{G} \rangle. \end{split} \tag{A13}$$

If the matrix element $[V(\rho_k)]_{(n_\rho n_\lambda, n'_\rho n'_\lambda); (m_{s_{1,2,3}}, m'_{s_{1,2,3}})}$ is independent of the spin operator, it can be written further as $[V(\rho_k)]_{(n_\rho n_\lambda, n'_\rho n'_\lambda)} \delta_{m_{s_1} m'_{s_1}} \delta_{m_{s_2} m'_{s_2}} \delta_{m_{s_3} m'_{s_3}}$. The matrix element $[V(\rho_k)]_{(n_\rho n_\lambda, n'_\rho n'_\lambda)}$ can be calculated with the help of the Jacobi coordinate transformation $(\rho_3, \lambda_3) \rightarrow (\rho_k, \lambda_k)$ (k=1, 2, 3), but it will be tedious in the framework of the GEM.

B. Infinitesimally-shifted Gaussian (ISG) basis functions

In the calculation of the Hamiltonian matrix elements of three-body systems, particularly when the Jacobi coordinate transformations are employed, integrations over all the radial and angular coordinates become laborious even with the Gaussian basis functions. This process can be simplified by introducing the ISG basis functions as

$$\phi_{nlm}^{G} = N_{nl}r^{l}e^{-\nu_{n}r^{2}}Y_{lm}(\mathbf{\bar{r}})$$

$$= N_{nl}\lim_{\varepsilon \to 0} \frac{1}{(\nu_{n}\varepsilon)^{l}} \sum_{\bar{l}=1}^{\bar{k}_{\max}} C_{lm,\bar{k}}e^{-\nu_{n}(\mathbf{r}-\varepsilon\mathbf{D}_{lm,\bar{k}})^{2}}, \qquad (B1)$$

where $r^l Y_{lm}(\bar{\mathbf{r}})$ is replaced by a set of coefficients $C_{lm,\bar{k}}$ and vectors $\mathbf{D}_{lm,\bar{k}}$. Thus, the Jacobi coordinate transformation only needs to be completed in the exponent section.

Considering an arbitrary matrix element $[V(\rho_k)]_{(n_\rho n_\lambda, n'_\rho n'_\lambda)}$, $V(\rho_k)$ is a scalar function of the radii ρ_k (k = 1, 2, 3, corresponding to JC-1, -2, -3, respectively), and the orbital angular momenta (l_ρ, m_ρ) , (l_λ, m_λ) , (l'_ρ, m'_ρ) , and (l'_λ, m'_λ) are defined under JC-3 in Fig. 1. Using the

ISG basis functions, we obtain

$$\begin{split} & [V(\rho_{k})]_{(n_{\rho}n_{\lambda},n'_{\rho}n'_{\lambda})} \\ &= \langle \phi^{G}_{n_{\rho_{3}}l_{\rho_{3}}m_{\rho_{3}}} \phi^{G}_{n_{\lambda_{3}}l_{\lambda_{3}}m_{\lambda_{3}}} |V(\rho_{k})| \phi^{G}_{n'_{\rho_{3}}l'_{\rho_{3}}m'_{\rho_{3}}} \phi^{G}_{n'_{\lambda_{3}}l'_{\lambda_{3}}m'_{\lambda_{3}}} \rangle \\ &= \{N_{nl}\}\{\lim_{\varepsilon \to 0} \frac{1}{(\nu_{n}\varepsilon)^{l}}\} \sum_{\{\bar{k}\}} \{C_{lm,\bar{k}}\} \langle e^{-\nu_{n_{\rho}}(\rho - \varepsilon_{\rho} \mathbf{D}_{\rho})} e^{-\nu_{n_{\lambda}}(\lambda - \varepsilon_{\lambda} \mathbf{D}_{\lambda})} | \\ & V(\rho_{k})| e^{-\nu_{n_{\rho'}}(\rho - \varepsilon_{\rho'} \mathbf{D}_{\rho'})} e^{-\nu_{n_{\lambda'}}(\lambda - \varepsilon_{\lambda'} \mathbf{D}_{\lambda'})} \rangle. \end{split} \tag{B2}$$

Here, $\{\cdots\}$ denotes the product of the contained elements. $\sum_{\tilde{k}}$ indicates sum over all the \tilde{k} values.

For the final integral of Eq. (B2), the following Jacobi coordinate transformations are performed,

$$\rho = \rho(\rho_k, \lambda_k)$$

$$\lambda = \lambda(\rho_k, \lambda_k)$$

$$d\rho d\lambda = ||J||d\rho_k d\lambda_k,$$
(B3)

with $\rho \equiv \rho_3$, $\lambda \equiv \lambda_3$, and k = 1, 2, 3. Here, |J| is the Jacobian determinant. The detailed derivation can be found in Ref. [54].

With the help of the ISG basis functions, the matrix elements of the Hamiltonian terms H_0 , G'_{ij} , \tilde{S}_{ij} , $\tilde{H}^{\text{tensor}}_{ij}$, and \tilde{H}^c_{ij} can be evaluated directly. The detailed results can be found in Ref. [44].

C. Spin-orbit terms

In Eq. (5) of Sec. II.A, the spin-orbit term $H_{ij}^{SO(\nu)}$ is given by

$$\begin{split} \tilde{H}_{ij}^{\text{so(v)}} &= \frac{\mathbf{s}_{i} \cdot (\mathbf{r}_{ij} \times \mathbf{p}_{i})}{2m_{i}^{2} r_{ij}} \frac{\partial \tilde{G}_{ii}^{\text{so(v)}}}{\partial r_{ij}} + \frac{\mathbf{s}_{j} \cdot (-\mathbf{r}_{ij} \times \mathbf{p}_{j})}{2m_{j}^{2} r_{ij}} \frac{\partial \tilde{G}_{jj}^{\text{so(v)}}}{\partial r_{ij}} + \\ &+ \frac{[\mathbf{s}_{i} \cdot (-\mathbf{r}_{ij} \times \mathbf{p}_{j}) + \mathbf{s}_{j} \cdot (\mathbf{r}_{ij} \times \mathbf{p}_{i})]}{m_{i} m_{j} r_{ij}} \frac{\partial \tilde{G}_{ij}^{\text{so(v)}}}{\partial r_{ij}} \\ &\equiv \tilde{H}_{ij}^{\text{so(v)ii}} + \tilde{H}_{ij}^{\text{so(v)jj}} + \tilde{H}_{ij}^{\text{so(v)ij}}. \end{split} \tag{C1}$$

The Jacobi coordinate transformations are expressed as

$$\mathbf{r}_{ij} = A_{rij}\boldsymbol{\rho} + B_{rij}\boldsymbol{\lambda},$$

$$\mathbf{p}_{i} = A_{pi}\mathbf{p}_{\rho} + B_{pi}\mathbf{p}_{\lambda},$$
(C2)

with $\rho_3 \equiv \rho$ and $\lambda_3 \equiv \lambda$. A_{rij} , B_{rij} , A_{pi} , and B_{pi} can be obtained by Eq. (13). Then, the spin-orbit term can be expressed in terms of the Jacobi coordinates ρ and λ , considering the first part of the spin-orbit term as an example:

$$\tilde{H}_{ij}^{SO(\nu)ii} = \frac{\partial \tilde{G}_{ii}^{so(\nu)}}{r_{ij}\partial r_{ij}} \left[\frac{A_{rij}A_{pi}}{2m_i^2} \mathbf{I}_{\rho} \cdot \mathbf{s}_i + \frac{B_{rij}B_{pi}}{2m_i^2} \mathbf{I}_{\lambda} \cdot \mathbf{s}_i + \frac{A_{rij}B_{pi}}{2m_i^2} (\boldsymbol{\rho} \times \mathbf{p}_{\lambda}) \cdot \mathbf{s}_i + \frac{B_{rij}A_{pi}}{2m_i^2} (\boldsymbol{\lambda} \times \mathbf{p}_{\rho}) \cdot \mathbf{s}_i \right].$$
(C3)

The terms proportional to $\lambda \times \mathbf{p}_{\rho}$ or $\boldsymbol{\rho} \times \mathbf{p}_{\lambda}$ are the three-body spin-orbit potentials, which have no contributions to the current calculations. The reason lies in the following result. According to the Wigner-Eckhart theorem, in the derivation of the matrix elements $\langle (\tilde{n}\alpha)_3^G | \frac{\partial \tilde{G}_{ij}^{\text{so}(\nu)}}{r_{ij}\partial r_{ij}} (\boldsymbol{\rho} \times \mathbf{p}_{\lambda}) \cdot \mathbf{s}_i | (\tilde{n}'\alpha)_3^G \rangle$, a reduced matrix element $\langle l_{\rho}l_{\lambda}L | \frac{\partial \tilde{G}_{ij}^{\text{so}(\nu)}}{r_{ij}\partial r_{ij}} \boldsymbol{\rho} \times \mathbf{p}_{\lambda} | l_{\rho}l_{\lambda}L \rangle$ appears and has the following form:

$$\langle l_{\rho}l_{\lambda}L||\frac{\partial \tilde{G}_{ii}^{\text{so}(v)}}{r_{ij}\partial r_{ij}}\boldsymbol{\rho} \times \mathbf{p}_{\lambda}||l_{\rho}l_{\lambda}L\rangle$$

$$= \sqrt{3}(2L+1)X\begin{pmatrix} l_{\rho} & l_{\lambda} & L\\ 1 & 1 & 1\\ l_{\rho} & l_{\lambda} & L \end{pmatrix} \langle l_{\rho}||\frac{\partial \tilde{G}_{ii}^{\text{so}(v)}}{r_{ij}\partial r_{ij}}\boldsymbol{\rho}||l_{\rho}\rangle\langle l_{\lambda}||\mathbf{p}_{\lambda}||l_{\lambda}\rangle,$$
(C4)

where $X(\cdots)$ is a 9-j coefficient. $\frac{\partial \tilde{G}_{ii}^{\text{so}(v)}}{r_{ij}\partial r_{ij}}$, ρ , and \mathbf{p}_{λ} are the irreducible spherical tensors of ranks 0, 1, and 1, respectively. The 9-j coefficient has an important property, *i.e.*, the result is one factor $(-1)^{\sum l_i}$ more than the original value, if any two rows (or columns) are permuted. Here, $\sum l_i$ indicates sum over all the nine elements. Hence, $X(\cdots)$ becomes zero in Eq. (C4).

Hence, the matrix element of $\tilde{H}_{ij}^{\mathrm{so}(\nu)ii}$ in a certain baryon state is expressed as

$$\langle (\tilde{n}, \alpha)_{3}^{G} | \tilde{H}_{ij}^{SO(\nu)ii} | (\tilde{n}', \alpha)_{3}^{G} \rangle$$

$$= \langle (\tilde{n}, \alpha)_{3}^{G} | \frac{\partial \tilde{G}_{ii}^{SO(\nu)}}{r_{ij} \partial r_{ij}} \left[\frac{A_{rij} A_{pi}}{2m_{i}^{2}} \boldsymbol{I}_{\rho} \cdot \mathbf{s}_{i} + \frac{B_{rij} B_{pi}}{2m_{i}^{2}} \boldsymbol{I}_{\lambda} \cdot \mathbf{s}_{i} \right] | (\tilde{n}', \alpha)_{3}^{G} \rangle$$

$$\equiv \sum_{(m_{\xi}, m_{\xi}')} \left\{ CG_{\xi} CG_{\xi'} \right\} \left[(\tilde{H}_{ij(1)}^{SO(\nu)ii})_{(n_{\rho}n_{\lambda}, n_{\rho}'n_{\lambda}'); (m_{s_{1,2,3}}, m_{s_{1,2,3}}')} + (\tilde{H}_{ij(2)}^{SO(\nu)ii})_{(n_{\rho}n_{\lambda}, n_{\rho}'n_{\lambda}'); (m_{s_{1,2,3}}, m_{s_{1,2,3}}')} \right], \tag{C5}$$

with

$$(\widetilde{H}_{ij(1)}^{SO(\nu)ii})_{(n_{\rho}n_{\lambda},n'_{\rho}n'_{\lambda});(m_{s_{1,2,3}},m'_{s_{1,2,3}})} = \left[\frac{\partial \widetilde{G}_{ii}^{so(\nu)}}{r_{ij}\partial r_{ij}} \left(\frac{A_{rij}A_{pi}}{2m_{i}^{2}} \mathbf{I}_{\rho} \cdot \mathbf{s}_{i} \right) \right]_{(n_{\rho}n_{\lambda},n'_{\rho}n'_{\lambda});(m_{s_{1,2,3}},m'_{s_{1,2,3}})}.$$
(C6)

The calculation of Eq. (C6) is performed in two steps. First, the algebraic calculation of $I_o \cdot s_i$ is performed,

$$(l_{\rho} \cdot \mathbf{s}_{i})|s_{1}m'_{s_{1}}\rangle|s_{2}m'_{s_{2}}\rangle|s_{3}m'_{s_{3}}\rangle|(n'_{\rho}l_{\rho}m'_{\rho})^{G}\rangle|(n'_{\lambda}l_{\lambda}m'_{\lambda})^{G}\rangle$$

$$= \sum_{\kappa} \xi_{\kappa} \times (|s_{1}m''_{s_{1}}\rangle|s_{2}m''_{s_{2}}\rangle|s_{3}m''_{s_{3}}\rangle|(n'_{\rho}l_{\rho}m''_{\rho})^{G}\rangle|(n'_{\lambda}l_{\lambda}m''_{\lambda})^{G}\rangle)_{\kappa}.$$
(C7)

Second, the remaining part with $\frac{\partial \tilde{G}_{ii}^{\text{so}(\nu)}}{r_{ij}\partial r_{ij}}$ in Eq. (C6) is calculated by means of the ISG basis functions and the Jacobi coordinate transformation $(\rho_3, \lambda_3) \rightarrow (\rho_k, \lambda_k)$ (k = 1, 2, 3). Thus, all the matrix elements of the spin-orbit terms can be computed rigorously.

D. Tables of results

Table D1. Contribution of each Hamiltonian term to the mass values (in MeV) for the 1*S*-, 1*P*-, and 1*D*-wave states of the Λ_c and Σ_c baryons with $\langle H_{\text{mode}} \rangle \equiv \langle H_0 + H^{\text{conf}} \rangle$ and $\langle H_{ij} \rangle \equiv \langle H \rangle - \langle (H - H_{ij}) \rangle$. The orbital excited states of the *ρ*-mode are marked in bold type.

$(l_{\rho}, l_{\lambda}) n L(J^{P})_{j}$	$\langle H_{\rm mode} \rangle$	$\{\langle H_{12}^t \rangle$	$\langle H_{23}^t \rangle$	$\langle H_{31}^t \rangle \}$	$\{\langle H^c_{12} \rangle$	$\langle H_{23}^c \rangle$	$\langle H_{31}^c \rangle \}$	$\{\langle H_{12}^{{ m SO}(v)} angle$	$\langle H_{23}^{{ m SO}(v)} \rangle$	$\langle H_{31}^{{ m SO}(v)} \rangle \}$	$\{\langle H_{12}^{{ m SO}(s)} \rangle$	$\langle H_{23}^{{ m SO}(s)} \rangle$	$\langle H_{31}^{\mathrm{SO}(s)} \rangle \}$	$\langle H \rangle$
							Λ_c							
$(0,0)1S(\frac{1}{2}^+)_0$	2464.30	{ 0	0	0 }	{ -176.49	0	0 }	{ 0	0	0 }	{ 0	0	0 }	2287.81
$(0,1)1P(\frac{1}{2}^{-})_1$	2781.78	{ 0	0	0 }	{ -162.80	0	0 }	{ 0	-15.52	-15.52 }	{ 0	3.84	3.84 }	2596.87
$(0,1)1P(\frac{3}{2}^{-})_1$	2781.78	{ 0	0	0 }	{ -161.42	0	0 }	{ 0	7.32	7.32 }	{ 0	-1.86	-1.86 }	2630.92
$(0,2)1D(\frac{3}{2}^+)_2$	3041.20	{ 0	0	0 }	{ -156.64	0	0 }	{ 0	-10.51	-10.51 }	{ 0	4.40	4.40 }	2872.53
$(0,2)1D(\frac{5}{2}^+)_2$	3041.20	{ 0	0	0 }	{ -156.61	0	0 }	{ 0	6.61	6.61 }	{ 0	-2.86	-2.86 }	2892.15
							Σ_c							
$(0,0)1S(\frac{1}{2}^+)_1$	2464.30	{ 0	0	0 }	{ 48.04	-27.58	-27.58 }	{ 0	0	0 }	{ 0	0	0 }	2456.24

TO 11 TO 1		C		
Table Di	-continued	trom	previous page	

(1 1) I (IP)	/11 \	(/IIt \	/11t \	/IIt \)	(/ U C \	/ LI C \	/ U C \)	(/77SO(v))	/ 7.7SO(v)	/ 7.7 SO(v) \)	(/77SO(s))	/ TTSO(s)	/ TTSO(s) \)	
$(l_{\rho}, l_{\lambda}) n L(J^{P})_{j}$		{(H ₁₂)	$\langle H_{23}^t \rangle$	$\langle H_{31}^t \rangle \}$	$\{\langle H_{12}^c \rangle$	$\langle H_{23}^c \rangle$	$\langle H_{31}^c \rangle \}$	$\{\langle H_{12}^{\mathrm{SO}(v)} \rangle$	$\langle H_{23}^{(3)} \rangle$	$\langle H_{31}^{\mathrm{SO}(v)} \rangle \}$	$\{\langle H_{12}^{\mathrm{SO}(s)} \rangle$	$\langle H_{23}^{{ m SO}(s)} \rangle$	$\langle H_{31}^{SO(s)} \rangle \}$	<i>⟨H⟩</i>
$(0,0)1S(\frac{3}{2}^+)_1$	2464.30	{ 0	0	0 }	{ 44.24	11.93	11.93 }	{ 0	0	0 }	{ 0	0	0 }	2533.92
$(0,1)1P(\frac{1}{2}^{-})_{0}$	2781.78	{ 0	0	0 }	{ 42.06	0	0 }	{ 0	-43.18	-43.18 }	{ 0	17.15	17.15 }	2773.06
$(0,1)1P(\frac{1}{2}^{-})_1$	2781.78	{ 0	0	0 }	{ 41.80	-4.72	-4.72 }	{ 0	-29.27	-29.27 }	{ 0	10.53	10.53 }	2778.02
$(0,1)1P(\frac{3}{2}^{-})_1$	2781.78	{ 0	0.74	0.74 }	{ 41.13	2.14	2.14 }	{ 0	-16.78	-16.78 }	{ 0	7.79	7.79 }	2810.40
$(0,1)1P(\frac{3}{2}^{-})_2$	2781.78	{ 0	-0.44	-0.44 }	{ 40.65	-6.02	-6.02 }	{ 0	9.38	9.38 }	{ 0	-6.02	-6.02 }	2816.13
$(1,0)1P(\frac{1}{2}^{-})_{1}$	2874.52	{ 0	0	0 }	{ -13.81	0	0 }	{ 0	-16.64	-16.64 }	{ 0	0	0 }	2828.13
$(0,1)1P(\frac{5}{2}^{-})_2$	2781.78	{ 0	1.38	1.38 }	{ 39.79	3.38	3.38 }	{ 0	25.01	25.01 }	{ 0	-10.68	-10.68 }	2862.97
$(1,0)1P(\frac{3}{2}^{-})_{1}$	2874.52	{ 0	0	0 }	{ -13.11	0	0 }	{ 0	8.07	8.07 }	{ 0	0	0 }	2877.37
$(0,2)1D(\frac{1}{2}^+)_1$	3041.20	{ 0	0	0 }	{ 39.77	1.72	1.72 }	{ 0	-42.03	-42.03 }	{ 0	23.07	23.07 }	3048.14
$(0,2)1D(\frac{3}{2}^+)_1$	3041.20	{ 0	-0.73	-0.73 }	{ 39.72	-0.79	-0.79 }	{ 0	-24.37	-24.37 }	{ 0	16.41	16.41 }	3062.98
$(0,2)1D(\frac{3}{2}^+)_2$	3041.20	{ 0	-0.14	-0.14 }	{ 39.28	-0.76	-0.76 }	{ 0	-18.78	-18.78 }	{ 0	9.95	9.95 }	3061.57
$(0,2)1D(\frac{5}{2}^+)_2$	3041.20	{ 0	0.46	0.46 }	{ 39.22	0.44	0.44 }	{ 0	-3.66	-3.66 }	{ 0	3.90	3.90 }	3082.51
$(0,2)1D(\frac{5}{2}^+)_3$	3041.20	{ 0	-0.64	-0.64 }	{ 38.59	-1.65	-1.65 }	{ 0	9.43	9.43 }	{ 0	-8.91	-8.91 }	3076.68
$(0,2)1D(\frac{7}{2}^+)_3$	3041.20	{ 0	1.29	1.29 }	{ 38.53	1.05	1.05 }	{ 0	23.17	23.17 }	{ 0	-15.54	-15.54 }	3101.93

Table D2. Calculated $\langle r_{\rho}^2 \rangle^{1/2}$, $\langle r_{\lambda}^2 \rangle^{1/2}$ (in fm) and mass values (in MeV) for the 1S-, 2S-, 3S-, 1P-, 2P-, and 1D-wave states of the $\Lambda_{c(b)}$ and $\Xi_{c(b)}$ baryons. The experimental data are also listed for comparison, taken by their isospin averages.

$(l_{\rho},l_{\lambda})nL(J^{P})_{j}$	$\langle r_{\rho}^2 \rangle^{1/2}$	$\langle r_{\lambda}^2 \rangle^{1/2}$	$M_{\rm cal.}$	Baryon/ $M_{\text{exp.}}/J_{\text{exp.}}^P$	$\langle r_{ ho}^2 angle^{1/2}$	$\langle r_{\lambda}^2 \rangle^{1/2}$	$M_{\rm cal.}$	Baryon/ $M_{\text{exp.}}/J_{\text{exp.}}^P$
			Λ_c				Λ_b	
$(0,0)1S(\frac{1}{2}^+)_0$	0.512	0.444	2288	$\Lambda_c^+/\sim 2286/\frac{1}{2}^+$ [2]	0.519	0.407	5622	$\Lambda_b^0/\sim 5620/\frac{1}{2}^+$ [2]
$(0,0)2S(\frac{1}{2}^+)_0$	0.631	0.786	2764	$\Lambda_c(2765)^+/\sim 2767/?$ [2]	0.599	0.716	6041	$\Lambda_b(6070)^0/\sim 6072/\frac{1}{2}^+$ [2]
$(0,0)3S(\frac{1}{2}^+)_0$	0.988	0.633	3022	-	0.953	0.677	6352	-
$(0,1)1P(\frac{1}{2}^{-})_1$	0.541	0.633	2597	$\Lambda_c(2595)^+/\sim 2592/\frac{1}{2}^-$ [2]	0.536	0.579	5899	$\Lambda_b(5912)^0/\sim 5912/\frac{1}{2}^{-}$ [2]
$(0,1)1P(\frac{3}{2}^{-})_1$	0.545	0.660	2631	$\Lambda_c(2625)^+/\sim 2628/\frac{3}{2}^-$ [2]	0.538	0.589	5913	$\Lambda_b(5920)^0/\sim 5920/\frac{3}{2}^{-}$ [2]
$(0,1)2P(\frac{1}{2}^{-})_1$	0.607	0.963	2990	$\Lambda_c(2910)^+/\sim$ 2914 /? [?] [2]	0.579	0.855	6239	-
$(0,1)2P(\frac{3}{2}^{-})_{1}$	0.602	0.991	3013	$\Lambda_c(2940)^+/\sim$ 2940 / $\frac{3}{2}^-$ [2]	0.577	0.861	6249	-
$(0,2)1D(\frac{3}{2}^+)_2$	0.555	0.826	2873	$\Lambda_c(2860)^+/\sim 2856/\frac{3}{2}^+$ [2]	0.543	0.748	6135	$\Lambda_b(6146)^0/\sim6146/\frac{3}{2}^+$ [2]
$(0,2)1D(\frac{5}{2}^+)_2$	0.556	0.851	2892	$\Lambda_c(2880)^+/\sim 2882/\frac{5}{2}^+$ [2]	0.544	0.758	6146	$\Lambda_b(6152)^0/\sim 6153/\frac{5}{2}^+$ [2]
			Ξ_c				Ξ_b	
$(0,0)1S(\frac{1}{2}^+)_0$	0.512	0.437	2479	$\Xi_c^{+,0}/\sim 2469/\frac{1}{2}^+$ [2]	0.518	0.400	5806	$\Xi_b^{0,-}/\sim$ 5795/ $\frac{1}{2}^+$ [2]
$(0,0)2S(\frac{1}{2}^+)_0$	0.645	0.768	2949	$\Xi_c(2970)^{+,0}/\sim 2966/\frac{1}{2}^+$ [2]	0.607	0.705	6224	$\Xi_b(6227)^{0,-}/\sim 6227/?$ [2]

TO 11 T	~ ~		1 0			
Table I	12-00	onfinii	ied fr	om n	revious	nage

$(l_{\rho},l_{\lambda})nL(J^{P})_{j}$	$\langle r_{\rho}^2 \rangle^{1/2}$	$\langle r_{\lambda}^2 \rangle^{1/2}$	$M_{\mathrm{cal.}}$	Baryon/ $M_{\text{exp.}}/J_{\text{exp.}}^P$	$\langle r_{\rho}^2 \rangle^{1/2}$	$\langle r_{\lambda}^2 \rangle^{1/2}$	$M_{\rm cal.}$	Baryon/ $M_{\text{exp.}}/J_{\text{exp.}}^P$
$(0,0)3S(\frac{1}{2}^+)_0$	0.968	0.607	3155	-	0.990	0.549	6480	-
$(0,1)1P(\frac{1}{2}^{-})_1$	0.544	0.628	2789	$\Xi_c(2790)^{+,0}/\sim 2793/\frac{1}{2}^{-}$ [2]	0.540	0.573	6084	$\Xi_b(6087)^0/\sim6087/\frac{3}{2}^{-}$ [2]
$(0,1)1P(\frac{3}{2}^{-})_1$	0.549	0.654	2820	$\Xi_c(2815)^{+,0}/\sim 2818/\frac{3}{2}^{-}$ [2]	0.543	0.582	6097	$\Xi_b(6100)^{0,-}/\sim6097/\frac{3}{2}^{-}$ [2]
$(0,1)2P(\frac{1}{2}^{-})_1$	0.616	0.950	3177	_	0.587	0.846	6422	-
$(0,1)2P(\frac{3}{2}^{-})_{1}$	0.612	0.977	3199	-	0.585	0.852	6431	-
$(0,2)1D(\frac{3}{2}^+)_2$	0.563	0.822	3061	$\Xi_c(3055)^+/\sim 3056/\frac{3}{2}^+$ [2]	0.552	0.742	6318	$\Xi_b(6327)^0/\sim 6327/?^?$ [2]
$(0,2)1D(\frac{5}{2}^+)_2$	0.564	0.845	3078	$\Xi_c(3080)^{+,0}/\sim 3079/\frac{5}{2}^+$ [2]	0.553	0.752	6328	$\Xi_b(6333)^0/\sim 6333/?^?$ [2]

Table D3. Calculated $\langle r_{\rho}^2 \rangle^{1/2}$, $\langle r_{\lambda}^2 \rangle^{1/2}$ (in fm) and mass values (in MeV) for the 1*s*-, 2*s*-, 3*s*-, 1*P*-, and 1*D*-wave states of the Σ_c and Σ_b baryons. The orbital excited states of the ρ -mode are marked in bold type. The experimental data are also listed for comparison, taken by their isospin averages.

$(l_{\rho},l_{\lambda})nL(J^{P})_{j}$	$\langle r_{\rho}^2 \rangle^{1/2}$	$\langle r_{\lambda}^2 \rangle^{1/2}$	$M_{\rm cal.}$	Baryon/ $M_{\text{exp.}}/J_{\text{exp.}}^P$	$\langle r_{ ho}^2 angle^{1/2}$	$\langle r_{\lambda}^2 \rangle^{1/2}$	$M_{\rm cal.}$	Baryon/ $M_{\text{exp.}}/J_{\text{exp.}}^P$
			Σ	<u> </u>			Σ_b	
$(0,0)1S(\frac{1}{2}^+)_1$	0.611	0.450	2456	$\Sigma_c(2455)^{++,+,0}/\sim 2453/\frac{1}{2}^+$ [2]	0.631	0.433	5821	$\Sigma_b^{+,-}/\sim 5813/\frac{1}{2}^+$ [2]
$(0,0)1S(\frac{3}{2}^+)_1$	0.645	0.493	2534	$\Sigma_c(2520)^{++,+,0}/\sim 2518/\frac{3}{2}^+$ [2]	0.645	0.449	5849	$\Sigma_b^{*+,-}/\sim 5833/\frac{3}{2}^+$ [2]
$(0,0)2S(\frac{1}{2}^+)_1$	0.841	0.732	2913	-	0.774	0.716	6226	-
$(0,0)2S(\frac{3}{2}^+)_1$	0.837	0.783	2967	-	0.770	0.734	6246	-
$(0,0)3S(\frac{1}{2}^+)_1$	0.945	0.718	3109	-	1.019	0.607	6439	-
$(0,0)3S(\frac{3}{2}^+)_1$	0.992	0.696	3127	-	1.041	0.594	6446	-
$(0,1)1P(\frac{1}{2}^{-})_0$	0.658	0.640	2773	-	0.652	0.593	6087	-
$(0,1)1P(\frac{1}{2}^{-})_1$	0.662	0.647	2778	$\Sigma_c(2800)^{++,+,0}/\sim 2800/?$ [2]	0.658	0.603	6092	$\Sigma_b(6097)^{+,-}/\sim6097/?$ [2]
$(0,1)1P(\frac{3}{2}^{-})_1$	0.670	0.672	2810	-	0.661	0.613	6105	-
$(0,1)1P(\frac{3}{2}^{-})_2$	0.678	0.688	2816	-	0.673	0.636	6113	-
$(1,0)1P(\frac{1}{2}^{-})_{1}$	0.857	0.486	2828	$\Sigma_c(2846)^0/\sim 2846/?$ [5]	-	-	-	-
$(0,1)1P(\frac{5}{2}^{-})_2$	0.689	0.731	2863	-	0.679	0.652	6133	-
$(1,0)1P(\frac{3}{2}^{-})_{1}$	0.875	0.505	2877	-	-	-	-	-
$(0,2)1D(\frac{1}{2}^+)_1$	0.683	0.817	3048	-	0.667	0.755	6330	-
$(0,2)1D(\frac{3}{2}^+)_1$	0.684	0.834	3063	-	0.668	0.761	6337	-
$(0,2)1D(\frac{3}{2}^+)_2$	0.690	0.846	3062	-	0.675	0.778	6334	-
$(0,2)1D(\frac{5}{2}^+)_2$	0.691	0.871	3083	-	0.677	0.789	6345	-
$(0,2)1D(\frac{5}{2}^+)_3$	0.700	0.891	3076	-	0.688	0.814	6338	-
$(0,2)1D(\frac{7}{2}^+)_3$	0.702	0.923	3102		0.690	0.828	6351	_

Table D4. Same as Table D3 but for the Ξ'_c and Ξ'_b baryons.

$(l_{\rho},l_{\lambda})nL(J^{P})_{j}$	$\langle r_{\rho}^2 \rangle^{1/2}$	$\langle r_{\lambda}^2 \rangle^{1/2}$	$M_{\rm cal.}$	Baryon/ $M_{\text{exp.}}/J_{\text{exp.}}^P$	$\langle r_{\rho}^2 \rangle^{1/2}$	$\langle r_{\lambda}^2 \rangle^{1/2}$	$M_{\rm cal.}$	Baryon/ $M_{\text{exp.}}/J_{\text{exp.}}^P$
			Ξ	Ξ_c'			Ξ_l'	,
$(0,0)1S(\frac{1}{2}^+)_1$	0.584	0.435	2589	$\Xi_c^{\prime+,0} /\sim 2578/\frac{1}{2}^+$ [2]	0.602	0.414	5944	$\Xi_b'(5935)^-/\sim 5935/\frac{1}{2}^+$ [2]
$(0,0)1S(\frac{3}{2}^+)_1$	0.614	0.474	2660	$\Xi_c(2645)^{+,0}/\sim 2645/\frac{3}{2}^+$ [2]	0.615	0.430	5971	$\Xi_b(5955)^{0,-}/\sim5954/\frac{3}{2}^+$ [2]
$(0,0)2S(\frac{1}{2}^+)_1$	0.809	0.714	3046	-	0.739	0.699	6351	-
$(0,0)2S(\frac{3}{2}^+)_1$	0.804	0.762	3096	-	0.735	0.715	6369	-
$(0,0)3S(\frac{1}{2}^+)_1$	0.925	0.685	3220	-	0.999	0.570	6543	-
$(0,0)3S(\frac{3}{2}^+)_1$	0.967	0.668	3237	-	1.017	0.561	6551	-
$(0,1)1P(\frac{1}{2})_0$	0.633	0.628	2906	$\Xi_c(2882)^0/\sim 2882/?$ [2]	0.629	0.578	6214	-
$(0,1)1P(\frac{1}{2}^{-})_1$	0.636	0.634	2912	-	0.633	0.587	6218	-
$(0,1)1P(\frac{3}{2}^{-})_1$	0.644	0.658	2941	$\Xi_c(2923)^{+,0}/\sim 2923/?$ [2, 22]	0.636	0.596	6230	-
$(0,1)1P(\frac{3}{2}^{-})_2$	0.649	0.670	2948	$\Xi_c(2930)^{+,0}/\sim 2941/?$ [2]	0.645	0.614	6237	-
$(1,0)1P(\frac{1}{2}^{-})_{1}$	0.828	0.473	2958	-	-	_	-	-
$(0,1)1P(\frac{5}{2}^{-})_2$	0.660	0.709	2990	-	0.650	0.629	6256	-
$(1,0)1P(\frac{3}{2})_1$	0.847	0.490	3004	-	-	_	_	-
$(0,2)1D(\frac{1}{2}^+)_1$	0.660	0.808	3177	$\Xi_c(3123)^+/\sim 3123/?^?$ [2]	0.647	0.742	6452	-
$(0,2)1D(\frac{3}{2}^+)_1$	0.662	0.824	3189	-	0.647	0.748	6458	-
$(0,2)1D(\frac{3}{2}^+)_2$	0.666	0.833	3190	-	0.653	0.761	6456	-
$(0,2)1D(\frac{5}{2}^+)_2$	0.668	0.856	3208	-	0.655	0.771	6466	-
$(0,2)1D(\frac{5}{2}^+)_3$	0.674	0.870	3207	-	0.663	0.790	6461	-
$(0,2)1D(\frac{7}{2}^+)_3$	0.676	0.899	3229	-	0.665	0.804	6473	-

Table D5. Same as Table D3 but for the Ω_c and Ω_b baryons.

$(l_{\rho},l_{\lambda})nL(J^{P})_{j}$	$\langle r_{\rho}^2 \rangle^{1/2}$	$\langle r_{\lambda}^2 \rangle^{1/2}$	$M_{\rm cal.}$	Baryon/ $M_{\text{exp.}}/J_{\text{exp.}}^P$	$\langle r_{\rho}^2 \rangle^{1/2}$	$\langle r_{\lambda}^2 \rangle^{1/2}$	$M_{\rm cal.}$	Baryon/ $M_{\text{exp.}}/J_{\text{exp.}}^P$
			Ω_c				Ω_b	
$(0,0)1S(\frac{1}{2}^+)_1$	0.549	0.417	2696	$\Omega_c^0/\sim 2695/\frac{1}{2}^+$ [2]	0.564	0.395	6043	$\Omega_b^-/{\sim}6045/rac{1}{2}^+$ [2]
$(0,0)1S(\frac{3}{2}^+)_1$	0.578	0.454	2765	$\Omega_c(2770)^0/\sim 2766/\frac{3}{2}^+$ [2]	0.576	0.409	6069	-
$(0,0)2S(\frac{1}{2}^+)_1$	0.775	0.686	3150	-	0.705	0.672	6448	-
$(0,0)2S(\frac{3}{2}^+)_1$	0.771	0.730	3198	$\Omega_c(3185)^0/\sim3185/?$ [2]	0.702	0.687	6465	-
$(0,0)3S(\frac{1}{2}^+)_1$	0.882	0.672	3325	$\Omega_c(3327)^0/\sim3327/?$ [2]	0.953	0.560	6641	-
$(0,0)3S(\frac{3}{2}^+)_1$	0.924	0.654	3339	-	0.973	0.549	6647	-
$(0,1)1P(\frac{1}{2}^{-})_0$	0.602	0.605	3009	$\Omega_c(3000)^0/\sim 3000/?$ [2]	0.595	0.552	6308	$\Omega_b(6316)^-/\sim 6315/?^?$ [2]
$(0,1)1P(\frac{1}{2}^{-})_1$	0.604	0.609	3015	-	0.599	0.560	6313	-

Table D5-continued from previous page

$(l_{\rho},l_{\lambda})nL(J^{P})_{j}$	$\langle r_{ ho}^2 angle^{1/2}$	$\langle r_{\lambda}^2 \rangle^{1/2}$	$M_{\rm cal.}$	Baryon/ $M_{\rm exp.}/J_{\rm exp.}^P$	$\langle r_{\rho}^2 \rangle^{1/2}$	$\langle r_{\lambda}^2 \rangle^{1/2}$	$M_{\rm cal.}$	Baryon/ $M_{\text{exp.}}/J_{\text{exp.}}^P$
$(0,1)1P(\frac{3}{2}^{-})_1$	0.612	0.633	3045	$\Omega_c(3050)^0/\sim3050/?^?$ [2]	0.602	0.570	6326	$\Omega_b(6330)^-/\sim 6330/?^?$ [2]
$(0,1)1P(\frac{3}{2}^{-})_2$	0.615	0.643	3052	-	0.608	0.586	6334	$\Omega_b(6340)^-/{\sim}6340/?^?$ [2]
$(1,0)1P(\frac{1}{2}^{-})_{1}$	0.792	0.459	3059	$\Omega_c(3065)^0/\sim 3065/?^2$ [2]	-	-	-	-
$(0,1)1P(\frac{5}{2}^{-})_2$	0.626	0.683	3095	$\Omega_c(3090)^0/\sim 3090/?$ [2]	0.614	0.601	6353	$\Omega_b(6350)^-/{\sim}6350/?^?$ [2]
$(1,0)1P(\frac{3}{2}^{-})_{1}$	0.813	0.479	3109	$\Omega_c(3120)^0/\sim3119/?^?$ [2]	-	-	_	-
$(0,2)1D(\frac{1}{2}^+)_1$	0.631	0.782	3278	-	0.616	0.713	6544	-
$(0,2)1D(\frac{3}{2}^+)_1$	0.633	0.801	3292	-	0.617	0.720	6552	-
$(0,2)1D(\frac{3}{2}^+)_2$	0.635	0.806	3293	-	0.621	0.731	6550	-
$(0,2)1D(\frac{5}{2}^+)_2$	0.637	0.831	3311	_	0.622	0.742	6561	-
$(0,2)1D(\frac{5}{2}^+)_3$	0.640	0.840	3310	_	0.627	0.759	6557	-
$(0,2)1D(\frac{7}{2}^+)_3$	0.642	0.871	3332		0.629	0.772	6570	_

Table D6. Deviations of the calculated masses of the 74 baryons from the measured ones [2, 5, 22]. Most of the deviations are less than 20 MeV. The arithmetic average deviation $(\sum_{i=1}^{n} |M_{\text{cal.}} - M_{\text{exp.}}|_i)/n$ is approximately 9.12 MeV. $M_{\text{exp.}}$ denotes the central value of the measured mass. "↑" indicates the same as above. $\Lambda_c(2910)^+$, $\Lambda_c(2940)^+$, and $\Xi_c(3123)^+$ are not included in the list.

Baryon (J^P)	$M_{\rm exp.}$	$(l_{\rho},l_{\lambda})nL(J^{P})_{j}$	$M_{\rm cal.}$	$M_{\rm cal.}-M_{\rm exp.}$	Baryon (J^P)	$M_{\rm exp.}$	$(l_{\rho},l_{\lambda})nL(J^{P})_{j}$	$M_{\rm cal.}$	$M_{\text{cal.}}-M_{\text{exp.}}$
$\Lambda_c^+(\frac{1}{2}^+)$	2286.46	$(0,0)1S(\frac{1}{2}^+)_0$	2288	1.54	$\Omega_c(2770)^0(\frac{3}{2}^+)$	2766	$(0,0)1S(\frac{3}{2}^+)_1$	2765	-1
$\Lambda_c(2595)^+(\frac{1}{2}^-)$	2592.25	$(0,1)1P(\frac{1}{2}^{-})_1$	2597	4.75	$\Omega_c(3000)^0(?^?)$	3000.46	$(0,1)1P(\frac{1}{2}^{-})_0$	3009	8.54
$\Lambda_c(2625)^+(\frac{3}{2}^-)$	2628	$(0,1)1P(\frac{3}{2}^{-})_1$	2631	3	$\Omega_c(3050)^0(?^?)$	3050.17	$(0,1)1P(\frac{3}{2}^{-})_1$	3045	-5.17
$\Lambda_c(2765)^+(?^?)$	2766.6	$(0,0)2S(\frac{1}{2}^+)_0$	2764	-2.6	$\Omega_c(3065)^0(?^?)$	3065.58	$(1,0)1P(\frac{1}{2}^{-})_1$	3059	-6.58
$\Lambda_c(2860)^+(\frac{3}{2}^+)$	2856.1	$(0,2)1D(\frac{3}{2}^+)_2$	2873	16.9	$\Omega_c(3090)^0(?^?)$	3090.15	$(0,1)1P(\frac{5}{2})_2$	3095	4.85
$\Lambda_c(2880)^+(\frac{5}{2}^+)$	2881.62	$(0,2)1D(\frac{5}{2}^+)_2$	2892	10.38	$\Omega_c(3120)^0(?^?)$	3118.98	$(1,0)1P(\frac{3}{2}^{-})_1$	3109	-9.98
$\Sigma_c(2455)^{++}(\frac{1}{2}^+)$	2453.97	$(0,0)1S(\frac{1}{2}^+)_1$	2456	2.03	$\Omega_c(3185)^0(?^?)$	3185	$(0,0)2S(\frac{3}{2}^+)_1$	3198	13
$\Sigma_c(2455)^+(\frac{1}{2}^+)$	2452.65	1	1	3.35	$\Omega_c(3327)^0(?^?)$	3327.1	$(0,0)3S(\frac{1}{2}^+)_1$	3325	-2.1
$\Sigma_c(2455)^0(\frac{1}{2}^+)$	2453.75	1	1	2.25	$\Lambda_b^0(\frac{1}{2}^+)$	5619.5	$(0,0)1S(\frac{1}{2}^+)_0$	5622	2.43
$\Sigma_c(2520)^{++}(\frac{3}{2}^+)$	2518.42	$(0,0)1S(\frac{3}{2}^+)_1$	2534	15.59	$\Lambda_b(5912)^0(\frac{1}{2})$	5912.16	$(0,1)1P(\frac{1}{2})_1$	5899	-13.2
$\Sigma_c(2520)^+(\frac{3}{2}^+)$	2517.4	↑	1	16.6	$\Lambda_b(5920)^0(\frac{3}{2}^-)$	5920.07	$(0,1)1P(\frac{3}{2}^{-})_1$	5913	-7.07
$\Sigma_c(2520)^0(\frac{3}{2}^+)$	2518.48	1	↑	15.52	$\Lambda_b(6070)^0(\frac{1}{2}^+)$	6072.3	$(0,0)2S(\frac{1}{2}^+)_0$	6041	-31.3
$\Sigma_c(2800)^{++}(??)$	2801	$(0,1)1P(\frac{1}{2}^{-})_1$	2778	-23	$\Lambda_b(6146)^0(\frac{3}{2}^+)$	6146.2	$(0,2)1D(\frac{3}{2}^+)_2$	6135	-11.2
$\Sigma_c(2800)^+(?^?)$	2792	1	↑	-14	$\Lambda_b(6152)^0(\frac{5}{2}^+)$	6152.5	$(0,2)1D(\frac{5}{2}^+)_2$	6146	-6.5
$\Sigma_c(2800)^0(?^?)$	2806	1	↑	-28	$\Sigma_h^+(\frac{1}{2}^+)$	5810.56	$(0,0)1S(\frac{1}{2}^+)_1$	5821	10.44
$\Sigma_c(2846)^0(?^?)$	2846	$(1,0)1P(\frac{1}{2}^{-})_1$	2828	-18	$\Sigma_b^-(\frac{1}{2}^+)$	5815.64	↑	1	5.36
$\Xi_c^+(\frac{1}{2}^+)$	2467.95	$(0,0)1S(\frac{1}{2}^+)_0(\mathbf{\bar{3}}_F)$	2479	11.05	$\Sigma_b^{*+}(\frac{3}{2}^+)$	5830.32	$(0,0)1S(\frac{3}{2}^+)_1$	5849	18.68
$\Xi_c^0(\frac{1}{2}^+)$	2470.44	1	↑	8.56	$\Sigma_{b}^{*-}(\frac{3}{2}^{+})$	5834.74	↑	1	14.26
$\Xi_c^{\prime +}(\frac{1}{2}^+)$	2578.2	$(0,0)1S(\frac{1}{2}^+)_1(6_F)$	2589	10.8	$\Sigma_b(6097)^+(?^?)$	6095.8	$(0,1)1P(\frac{1}{2})_1$	6092	-3.8
$\Xi_c^{\prime 0}(\frac{1}{2}^+)$	2578.7	1	1	10.3	$\Sigma_b(6097)^-(?^?)$	6098.0	↑	1	-6.0
$\Xi_c(2645)^+(\frac{3}{2}^+)$	2645.1	$(0,0)1S(\frac{3}{2}^+)_1(6_F)$	2660	14.9	$\Xi_b^-(\frac{1}{2}^+)$	5797	$(0,0)1S(\frac{1}{2}^+)_0(6_F)$	5806	9

Table D6-continued from previous page

Baryon (J^P)	$M_{\rm exp.}$	$(l_{\rho},l_{\lambda})nL(J^{P})_{j}$	$M_{\rm cal.}$	$M_{\rm cal.}-M_{\rm exp.}$	Baryon (J^P)	$M_{\rm exp.}$	$(l_{\rho}, l_{\lambda}) n L(J^{P})_{j}$	$M_{\rm cal.}$	$M_{\rm cal.}-M_{\rm exp.}$
$\Xi_c(2645)^0(\frac{3}{2}^+)$	2645.7	1	1	14.3	$\Xi_b^0(\frac{1}{2}^+)$	5791.7	↑	1	14.3
$\Xi_c(2790)^+(\frac{1}{2}^-)$	2791.9	$(0,1)1P(\frac{1}{2}^{-})_{1}(\mathbf{\bar{3}}_{F})$	2789	-2.9	$\Xi_b(5935)^-(\frac{1}{2}^+)$	5934.9	$(0,0)1S(\frac{1}{2}^+)_1(6_F)$	5944	9.1
$\Xi_c(2790)^0(\frac{1}{2}^-)$	2793.9	↑	1	-4.9	$\Xi_b(5945)^0(\frac{3}{2}^+)$	5952.3	$(0,0)1S(\frac{3}{2}^+)_1(6_F)$	5971	18.7
$\Xi_c(2815)^+(\frac{3}{2}^-)$	2816.51	$(0,1)1P(\frac{3}{2}^{-})_1(\mathbf{\bar{3}}_F)$	2820	3.49	$\Xi_b(5955)^-(\frac{3}{2}^+)$	5955.5	1	1	15.5
$\Xi_c(2815)^0(\frac{3}{2}^-)$	2819.79	↑	1	0.21	$\Xi_b(6087)^-(\frac{3}{2}^-)$	6087	$(0,1)1P(\frac{1}{2}^{-})_{1}(\mathbf{\bar{3}}_{F})$	6084	-3
$\Xi_c(2882)^0(??)$	2882	$(0,1)1P(\frac{1}{2}^{-})_0(6_F)$	2906	24	$\Xi_b(6095)^0(\frac{3}{2}^-)$	6095.1	$(0,1)1P(\frac{3}{2}^{-})_{1}(\mathbf{\bar{3}}_{F})$	6097	1.9
$\Xi_c(2923)^+(?^?)$	2922.8	$(0,1)1P(\frac{3}{2}^{-})_1(6_F)$	2941	18.2	$\Xi_b(6100)^-(\frac{3}{2}^-)$	6099.8	1	1	-2.8
$\Xi_c(2923)^0(??)$	2923.2	1	1	17.8	$\Xi_b(6227)^-(??)$	6227.9	$(0,0)2S(\frac{1}{2}^+)_0(\mathbf{\bar{3}}_F)$	6224	-3.9
$\Xi_c(2930)^+(?^?)$	2942	$(0,1)1P(\frac{3}{2}^{-})_2(6_F)$	2948	6	$\Xi_b(6227)^0(??)$	6226.8	1	1	-2.8
$\Xi_c(2930)^0(??)$	2938.55	1	1	9.45	$\Xi_b(6327)^0(??)$	6327.28	$(0,2)1D(\frac{3}{2}^{-})_2(\mathbf{\bar{3}}_F)$	6318	-9.28
$\Xi_c(2970)^+(\frac{1}{2}^+)$	2964.3	$(0,0)2S(\frac{1}{2}^+)_0(\mathbf{\bar{3}}_F)$	2949	-15.3	$\Xi_b(6333)^0(??)$	6332.69	$(0,2)1D(\frac{5}{2}^{-})_2(\mathbf{\bar{3}}_F)$	6328	-4.69
$\Xi_c(2970)^0(\frac{1}{2}^+)$	2965.9	1	1	-16.9	$\Omega_b^-({1\over2}^+)$	6045.8	$(0,0)1S(\frac{1}{2}^+)_1$	6043	-2.8
$\Xi_c(3055)^+(\frac{3}{2}^+)$	3055.9	$(0,2)1D(\frac{3}{2}^+)_2(\mathbf{\bar{3}}_F)$	3061	5.1	$\Omega_b(6316)^-(??)$	6315.6	$(0,1)1P(\frac{1}{2}^{-})_0$	6308	-7.6
$\Xi_c(3080)^+(\frac{5}{2}^+)$	3077.2	$(0,2)1D(\frac{5}{2}^+)_2(\mathbf{\bar{3}}_F)$	3078	0.8	$\Omega_b(6330)^-(??)$	6330.3	$(0,1)1P(\frac{3}{2}^{-})_1$	6326	-4.3
$\Xi_c(3080)^0(\frac{5}{2}^+)$	3079.9	↑	1	-1.9	$\Omega_b(6340)^-(??)$	6339.7	$(0,1)1P(\frac{3}{2}^{-})_2$	6334	-5.7
$\Omega_c^0(\frac{1}{2}^+)$	2695.3	$(0,0)1S(\frac{1}{2}^+)_1$	2696	0.7	$\Omega_b(6350)^-(?^?)$	6349.8	$(0,1)1P(\frac{5}{2}^-)_2$	6353	3.2

References

- [1] F. Gross, E. Klempt, S. J. Brodsky *et al.*, Eur. Phys. J. C **83**, 1125 (2023), arXiv: 2212.11107[hep-ph]
- [2] S. Navas et al. (Particle Data Group), Phys. Rev. D 110(3), 030001 (2024)
- [3] R. Mizuk et al. (Belle Collaboration), Phys. Rev. Lett. 94, 122002 (2005), arXiv: hep-ex/0412069[hep-ex]
- [4] B. Aubert *et al.* (BABAR Collaboration), Phys. Rev. D 77, 012002 (2008), arXiv: 0710.5763[hep-ex]
- [5] B. Aubert et al. (BABAR Collaboration), Phys. Rev. D 78, 112003 (2008), arXiv: 0807.4974[hep-ex]
- [6] R. Aaij et al. (LHCb Collaboration), JHEP 05, 030 (2017), arXiv: 1701.07873[hep-ex]
- [7] R. Aaij *et al.* (LHCb Collaboration), Phys. Rev. Lett. **118**(18), 182001 (2017), arXiv: 1703.04639[hep-ex]
- [8] J. Yelton *et al.* (Belle Collaboration), Phys. Rev. D **97**(5), 051102 (2018), arXiv: 1711.07927[hep-ex]
- [9] Y. B. Li *et al.* (Belle Collaboration), Eur. Phys. J. C **78**(3), 252 (2018), arXiv: 1712.03612[hep-ex]
- [10] R. Aaij *et al.* (LHCb Collaboration), Phys. Rev. Lett. **121**(7), 072002 (2018), arXiv: 1805.09418[hep-ex]
- [11] Y. B. Li *et al.* (Belle Collaboration), Eur. Phys. J. C **78**, 928 (2018), arXiv: 1806.09182[hep-ex]
- [12] R. Aaij *et al.* (LHCb Collaboration), Phys. Rev. Lett. **122**(1), 012001 (2019), arXiv: 1809.07752[hep-ex]
- [13] R. Aaij *et al.* (LHCb Collaboration), Phys. Rev. Lett. **124**(8), 082002 (2020), arXiv: 2001.00851[hep-ex]
- [14] R. Aaij *et al.* (LHCb Collaboration), Phys. Rev. Lett. **124**, 222001 (2020), arXiv: 2003.13649[hep-ex]
- [15] R. Aaij et al. (LHCb Collaboration), Phys. Rev. Lett. 103(1), 012004 (2021), arXiv: 2010.14485[hep-ex]

- [16] R. Aaij et al. (LHCb Collaboration), Phys. Rev. D 104(9), L091102 (2021), arXiv: 2107.03419[hep-ex]
- [17] Y. B. Li et al. (Belle Collaboration), Phys. Rev. Lett. 130(3), 031901 (2023), arXiv: 2206.08822[hep-ex]
- [18] R. Aaij *et al.* (LHCb Collaboration), Phys. Rev. D **108**, 012020 (2023), arXiv: 2211.00812[hep-ex]
- [19] R. Aaij *et al.* (LHCb Collaboration), Phys. Rev. Lett. **131**(13), 131902 (2023), arXiv: 2302.04733[hep-ex]
- [20] R. Aaij et al. (LHCb Collaboration), Phys. Rev. Lett. 131(17), 171901 (2023), arXiv: 2307.13399[hep-ex]
- [21] R. Aaij et al. (LHCb Collaboration), arXiv: 2409.05440 [hep-ex]
- [22] R. Aaij *et al.* (LHCb Collaboration), arXiv: 2502.18987 [hep-ex]
- [23] H. Y. Cheng, Chin. J. Phys. **78**, 324 (2022), arXiv: 2109.01216[hep-ph]
- [24] H. X. Chen, W. Chen, X. Liu *et al.*, Rept. Prog. Phys. **86**(2), 026201 (2023), arXiv: 2204.02649[hep-ph]
- [25] V. Crede and J. Yelton, Rept. Prog. Phys. 87(10), 106301 (2024)
- [26] S. Godfrey and N. Isgur, Phys. Rev. D 32, 189 (1985)
- [27] S. Capstick and N. Isgur, Phys. Rev. D 34, 2809 (1986)
- [28] X. Z. Weng, W. Z. Deng, and S. L. Zhu, Phys. Rev. D 110(5), 056052 (2024), arXiv: 2405.19039[hep-ph]
- [29] S. Capstick and W. Roberts, Prog. Part. Nucl. Phys. 45, S241 (2000), arXiv: 0008028[nucl-th]
- [30] N. Isgur and M. B. Wise, Phys. Rev. Lett. **66**, 1130 (1991)
- [31] H. Georgi, Phys. Lett. B 240, 447 (1990)
- [32] E. Eichten and B. R. Hill, Phys. Lett. B **234**, 511 (1990)
- [33] W. Roberts and M. Pervin, Int. J. Mod. Phys. A 23, 2817 (2008), arXiv: 0711.2492[nucl-th]
- [34] D. Ebert, R. N. Faustov, and V. O. Galkin, Phys. Rev. D 84,

- 014025 (2011), arXiv: 1105.0583[hep-ph]
- [35] J. R. Zhang, Phys. Rev. D **89**(9), 096006 (2014), arXiv: 1212.5325[hep-ph]
- [36] H. Y. Cheng, arXiv: 1508.07233[hep-ph]
- [37] H. X. Huang, J. L. Ping, and F. Wang, Phys. Rev. D **97**(3), 034027 (2018), arXiv: 1704.01421[hep-ph]
- [38] Z. G. Wang, Nucl. Phys. B **926**, 467 (2018), arXiv: 1705.07745[hep-ph]
- [39] Q. F. Lü and X. H. Zhong, Phys. Rev. D 101(7), 014017 (2020), arXiv: 1910.06126[hep-ph]
- [40] Z. G. Wang and H. J. Wang, Chin. Phys. C **45**(1), 013109 (2021), arXiv: 2006.16776[hep-ph]
- [41] A. Kakadiya, Z. Shah, and A. K. Rai, Int. J. Mod. Phys. A **37**(11n12), 2250053 (2022), arXiv: 2202.12048[hep-ph]
- [42] Q. Xin, Z. G. Wang, and F. Lü, Chin. Phys. C 47, 093106 (2023), arXiv: 2306.05626[hep-ph]
- [43] E. Ortiz-Pacheco and R. Bijker, Phys. Rev. D **108**(5), 054014 (2023), arXiv: 2307.04939[hep-ph]
- [44] G. L. Yu, Z. Y. Li, Z. G. Wang *et al.*, Nucl. Phys. B **990**, 116183 (2023), arXiv: 2206.08128[hep-ph]
- [45] Z. Y. Li, G. L. Yu, Z. G. Wang *et al.*, Chin. Phys. C **47**, 073105 (2023), arXiv: 2207.04167[hep-ph]
- [46] G. L. Yu, Z. Y. Li, Z. G. Wang et al., Eur. Phys. J. A 59,

- 126 (2023), arXiv: 2211.00510[hep-ph]
- [47] Z. Y. Li, G. L. Yu, Z. G. Wang *et al.*, Mod. Phys. Lett. A **38**(08n09), 2350052 (2023), arXiv: 2210.13085[hep-ph]
- [48] Z. Y. Li, G. L. Yu, Z. G. Wang *et al.*, Int. J. Mod. Phys. A **38**(18n19), 2350095 (2023), arXiv: 2211.15111[hep-ph]
- [49] Z. Y. Li, G. L. Yu, Z. G. Wang *et al.*, Eur. Phys. J. C **84**(2), 106 (2024), arXiv: 2311.08251[hep-ph]
- [50] Z. Y. Li, G. L. Yu, Z. G. Wang *et al.*, Eur. Phys. J. C **84**(12), 1310 (2024), arXiv: 2405.16162[hep-ph]
- [51] N. Isgur and G. Karl, Phys. Rev. D 18, 4187 (1978)
- [52] N. Isgur, Phys. Rev. D 62, 014025 (2000), arXiv: hep-ph/9910272[hep-ph]
- [53] M. Kamimura, Phys. Rev. A 38, 621 (1988)
- [54] E. Hiyama, Y. Kino, and M. Kamimura, Prog. Part. Nucl. Phys. 51, 223 (2003)
- [55] Q. F. Lü, D. Y. Chen, and Y. B. Dong, Phys. Rev. D **102**, 034012 (2020), arXiv: 2006.08087[hep-ph]
- [56] H. H. Zhong, M. S. Liu, R. H. Ni et al., Phys. Rev. D 110(11), 116034 (2024), arXiv: 2409.07998[hep-ph]
- [57] Z. L. Zhang, Z. W. Liu, S. Q. Luo *et al.*, Phys. Rev. D **107**(3), 034036 (2023), arXiv: 2210.17188[hep-ph]
- [58] B. Chen, S. Q. Luo, and X. Liu, Eur. Phys. J. C **81**(5), 474 (2021), arXiv: 2101.10806[hep-ph]